ASTRONOMY & ASTROPHYSICS
SUPPLEMENT SERIES

NOVEMBER I 1990, PAGE 1101

Astron. Astrophys. Suppl. Ser. **85**, 1101-1125 (1990)

Rotational integral cross sections and rate coefficients of HD scattered by He and H2

J. Schaefer

Max-Planck-Institut für Physik und Astrophysik, Institut für Astrophysik, Karl-Schwarzschild-Str. 1, 8046 Garching, F.R.G.

Received Febuary 12; accepted March 30, 1990

Abstract. — The previously described interaction potentials of HD-He and HD-H2 have been used in close coupled scattering calculations for providing integral cross sections and subsequently rate coefficients at temperatures up to 600 K (HD-He) and 300 K (HD-H2). Errors of about 10% for the leading low angular momentum transitions of HD have been estimated mainly from previous tests of the original H2-He and H2-H2 interaction potentials. Angular momentum transfer cross sections of the HD-H2 system have been found much smaller than the leading ones, and their possible errors could be relatively large due to neglected details of anisotropic short range interactions. Some interesting similarities and differences of $\Delta j_{HD} = 1$ cross sections of both systems have been discussed.

Key words: molecular processes — interstellar molecules — planetary atmospheres.

1. Introduction.

Integral cross sections and rate coefficients of HD transitions at low angular momenta in collisions with H2 and He could become interesting in the near future for the modelling of pre-galactic clouds and planetary atmospheres when the planned satellite bound observations of HD lines in the far infrared can be done successfully. Data as accurate as possible should certainly be used for this application. It is therefore quite interesting to show how accurate the theoretical data pressently can be.

Previous theoretical work on rotational rate coefficients of HD should be mentioned first. Green (1974) has studied the HD-He system and showed essentially the same results as ours for the rate coefficients of the leading transitions, up to room temperature. He had utilized the Shafer-Gordon (1973) potential of H2-He which is the best non-spherical multiple property fit available for this system. Some consequences of the differences between this potential fit and the ab initio potential used in this work show up in $\Delta j = 2$ cross sections and rate coefficients. The famous potential fit had not been available in an earlier attempt of Itikawa and Takayanagi (1972) who obtained a roughly 10% different $j = 0 \rightarrow 1$ rate coefficient at low temperatures giving a small disagreement in the comparison with the measured relaxation times (or the equivalent $\sigma(0001)$ cross section).

The only previous attempt known to the author of computing rotational rate coefficients of HD in collisions with H2 has been published by Chu (1975). Unfortunately, the results obtained at this time were suffering from a lack of knowledge about the interaction potential of the HD-H2 system. Despite this problem some rate coefficients of the leading HD transitions, at low temperatures up to about 60 K, are in surprisingly good agreement with our results. The main reason for this is the use of an empirical isotropic potential fit of Farrar *et al.* (1972) which determines mainly the V_{000} and the V_{101} term of the HD-H2 potential. Rather large deviations of our results have been found at 300 K. This indicates relative strong coupling at larger collision energies which could not be handled properly at this time.

Deficiencies of the interaction potential and especially of the anisotropic terms are usually the main source of errors of rotationally inelastic cross sections and rate coefficients. Tests of the potential can be done if there are accurately measured quantities available which are determined by these data, e.g. rotational relaxation times. Alternatively, we can test the potentials also by comparing similar sensitive quantities, sampled in the same interaction range, in order to derive plausible estimates of the errors. Since we can certainly assume validity of the Born-Oppenheimer approximation, the electronic potential energy surfaces (PES) are exactly the same for the H2-He and HD-He systems, as well as for H2-H2 and HD-H2. The different interaction potential expansions are due to the replacement of H2 by HD, i.e., the shift of the molecular center of mass point in the latter.

Send offprint requests to:

Comparisons of calculated and measured quantities of H2-He have shown the high quality of the full non-spherical interaction potential, while some sensitive tests for HD-He provided proof for the proper substitution of H2 by HD. Many measured data have been used for tests of the spherical and the full non-spherical H2-H2 potential, and we found quantitative agreement in the comparisons, but much less measurements have been done for the isotopic HD-H2 system that could be used for showing the proper substitution of H2 by HD again. Both PES and their tests as well as estimates of remaining errors due to the potential will be briefly dicussed in section 2.

Some other errrors are due to the applied theoretical (numerical) procedures. The scattering matrices have been calculated numerically by applying the *close coupled* formalism as introduced by Arthurs and Dalgarno (1960). Since we have confined our computational efforts to the less expensive calculations, we could avoid the use of approximate scattering formalisms which apply reasonable restrictions to the *close coupled* differential equation systems and thereby include some extra errors. Some errors are unavoidable because of economical reasons: the finite set of asymptotic basis functions has been limited reasonably. Test calculations have shown the amount of convergence reached for the cross sections. Minor important errors occurred in subsequently obtained quantities, e.g., some low temperature rate coefficients include errors due to interpolations applied to the cross section curves vs. energy prior to the energy averaging. Estimates of such potential-independent errors will be discussed in section 3.

Both the H2-He and the H2-H2 PES are in general weakly anisotropic. The same kind of substitution of a H2 molecule by a HD molecule has been applied to the two PES which gave the leading anisotropic potential term among others for each substituted system. As a result, we found common features for the two systems that will be discussed in section 4. Conclusions will complete the paper in section 5.

2. Estimated errors due to the interaction potentials.

The HD-He interaction potential has been transformed from a 3-term Legendre expansion of the interaction potential of H2-He which has been combined from the ab initio results published by Meyer *et al.* (1980). These two potentials share the isotropic term approximately, while the anisotropies are quite different. For a brief and qualitative comparison we show the two potentials in Figure 1 as obtained at $r_{H2}=r_{HD} = 1.449$ a.u. Both potentials could be tested quite extensively in comparisons of theoretical and measured quantities (Köhler *et al.*, 1983a, Schaefer *et al.*, 1985). However, rotationally inelastic cross sections of HD-He could be tested only at rather low collision energies. Three measured points of the differential $\Delta j = 1$ cross section at 30.9 me V relative kinetic energy (Gentry *et al.*, 1977) gave complete agreement with theoretical results (Schaefer *et al.*, 1985). The measured sound absorption relaxation times at temperatures between 20.4 K (10% exp. error) and 42.6 K (7% exp. error) (Prangsma *et al.*, 1970) as well as the equivalent rotational relaxation cross sections $\sigma(0001)$ have been reproduced within 10% error bars (Schaefer *et al.*, 1985). Measurements at higher temperatures are not available for the direct test. A similar sensitive anisotropy dependent cross section, the production cross section of the tensor polarization of rotational angular momenta in a viscous flow, $\sigma_{T\eta}$, measured at room temperature, has been quantitatively reproduced (Köhler *et al.*, 1983a). It is the only very sensitive test of the non-spherical interaction potential part of HD-He at room temperature. Many tests have been made in application of the Waldmann-Snider kinetic theory describing magnetic field effects in transport and orientation phenomena (Köhler *et al.*, 1983a). Quantitative agreement (deviations $< 10\%$) has been achieved with the available measurements (Senftleben-Beenakker effects) of Beenakker, Knaap and coworkers in the Molecular Physics Group in Leiden. Almost all of these tests have probed mainly the isotropic H2-He potential because this determines mainly the V_0 and the V_1 term of HD-He. Sensitive anisotropy dependent quantities of the H2-He system as rotational and NMR relaxation, depolarized Rayleigh and rotational Raman line shape cross sections have been tested successfully (Schaefer *et al.*, 1985) which provides proof for a very good PES prior to the determination of the isotopically substituted potential. Most of the measurements used there belonged to the thesis work of Hermans (1983).

No serious shortcoming of this PES could be found which really required an empirical improvement. This can be said based on uncertainties that are likely contained in a few of the measured data (Dilling *et al.*, 1989). However, more accurate measurements could still provide evidence for minor improvements of the PES. Presently, there has been only one exceptional accurate series of data, the NMR relaxation times of ortho-H2 in He gas, measured by Lemaire *et al.* (1984) up to room temperature which really could have shown a shortcoming of our H2-He potential and especially of its anisotropy, but even these very accurate data have been reproduced quantitatively.

In spite of the missing direct tests of our listed data it seems presently reasonable to estimate a maximum error of 10% - due to the interaction potential - according to the generally found maximum of deviations of the calculated quantities compared with measurements. Admittedly, there is no direct link between the errors of the various quantities, but a few of those are comparable sensitive with regard to the anisotropy. The error estimate holds especially for the dominating ($\Delta j = 1$, governed by the V_1 term) rate coefficients at temperatures up to 300 K. Theory could be better, but the few direct measurements require this error bar. By taking other measurements into account we can still estimate something else reasonably: Since the V_2 term of the

HD-He potential is essentially determined by the V_0 and V_2 terms of the H2-He potential and both could be tested very successfully, we may assume also about 10% errors - due to the potential - for the $\Delta j = 2$ cross sections, especially at the smaller collision energies, and rate coefficients up to 300 K. There is no direct experimental proof giving credit to this estimate, as e.g. a relaxation cross section measured at room temperature with an error of $\pm 1\%$. The $\Delta j = 2$ cross sections and rate coefficients are certainly more sensitive than the dominating ones, especially to possible improvements of the V_4 term of H2-He at small center of mass distances and to vibrationally inelastic effects at larger collision energies. No error estimates can be made for the really small rate coefficients. Additional errors not depending upon the interaction potential will be shown to be about 10% for the $\Delta j = 1$ and approximately twice as large for the $\Delta j = 2$ cross sections at larger collision energies, due to the basis expansions and numerical procedures.

Keeping all these errors in mind, an extension of the rate coefficients up to 600 K temperature seems still reasonable. However, we know from previous tests (Köhler *et al.*, 1983a) that 300 K is about the limit for the neglect of $j > 4$ contributions in effective cross sections, i.e., cross sections and rate coefficients of initial and final higher rotational HD states play an increasingly important role above room temperature. We should presume also contributions from vibrationally inelastic collisions below 600 K, adding to the effective cross sections and improving some of our integral cross sections - especially the smaller ones - at relatively large collision energies.

A comparable amount of accuracy for the more complex H2-H2 and HD-H2 systems has been reached after some steps of improvement. Discussions of previous potential versions and conclusions derived from quite a number of comparisons with measurements can be found in recent papers (Monchick *et al.*, 1987; Schaefer *et al.*, 1989) and references mentioned therein. The spherical and three anisotropic terms of the potential surface of H2-H2 are the important terms of an expansion in triple products of spherical harmonics. The leading two anisotropic terms, V_{202} and V_{022} (which are equal in the rigid rotor approximation due to the symmetry of the system), are responsible for direct $\Delta j_i = 2$ transitions of the first and the second molecule, respectively, while the third anisotropic term, V_{224}, determined asymptotically by the quadrupole-quadrupole interaction, contributes to rotationally inelastic transitions only when both molecules are rotating initially and/or finally.

The isotropic potential has been empirically improved finally (Schaefer *et al.*, 1989) by starting from a previous non-spherical potential version ("M80") that has been derived entirely from quantum chemical ab initio results of Meyer and Liu (remark 1). Then the anisotropy of the previous potential had to be transferred somehow to this new fit curve ("F84"), in order to conserve the previously tested high quality of cross sections of rotationally inelastic H2 transitions and the corresponding rate coefficients. This could be done successfully by conserving the relative anisotropies. We had found out empirically in previous studies (Buck *et al.*, 1981, 1983) that ratios of inelastic and elastic differential cross sections at fixed scattering angle had been conserved in small shifts of the complete potential along the intermolecular separation coordinate. Since the fit has been obtained from the ab initio V_{000} term by using scaling procedures, the same scaling could simply be applied to all potential terms. After this, the fit potential version F84 gives now integral inelastic cross sections with small deviations compared to the results obtained from the previous M80 potential. Proof is provided in Figure 2 by showing again one of the most sensitive anisotropy dependent cross sections, $\sigma(0001)$, for the rotational relaxation of para-hydrogen, up to $T = 200$ K. This cross section includes all rates of inelastic transitions between pairs of angular momenta (0,0), (0,2), and (2,2). The test results of Figure 2 can be compared with previous results derived from the M80 potential (Köhler *et al.*, 1983b); there is a general decrease of 2 - 3%. Both sets of data show agreement with the measurements of Jonkman *et al.* (1968) within the drawn 10% error bars. The claimed experimental errors are 3.2% at 77 K, 1% at 90.5 K, 2% at 111.5 K, and 1% at 170 K which in general indicates a slightly too small anisotropy at these lower temperatures. Another measured value at room temperature could be reproduced quantitatively ($\pm 1\%$) by using a converged set of rate coefficients (remark 2).

The expansion coefficient functions of the HD-H2 potential have been determined from 41 carefully chosen HD-H2 configurations which gives 41 potential expansion terms out of which twelve have been used in the collision calculations, namely V_{000}, V_{101}, V_{121}, V_{123}, V_{303}, V_{323}, V_{325}, V_{022}, V_{202}, V_{222}, V_{224} and V_{404}. These terms had been selected by using the criterion that their absolute magnitude at 3.0 a.u. center of mass distance was larger than 4.5×10^{-5} a.u. The quite reasonable assumption was that any additional anisotropy of this order of magnitude does not contribute significantly to the dynamics of the system. The huge number of terms involved in the transformation of the potential has been found necessary for reaching satisfying completeness of the twelve terms finally retained.

While the full non-spherical H2-H2 interaction potential could be tested quite extensively and successfully, there was no measurement available for direct tests of integral cross sections and rate coefficients of HD-H2. The only sensitive test of this potential could be done in comparisons with measured differential cross sections of HD-D2 obtained in crossed beam experiments by Buck *et al.* (1983) Success has been achieved with the final H2-H2 potential version and the just described HD-H2 potential. This comparison has been shown in a previous paper (Monchick *et al.*, 1987) from which we infer - for just one *integral* $\Delta j_{HD} = 1$ cross section - an error below 10%. As far as the detailed analysis of this measurement has shown, the main part of the

anisotropy of the HD-H2 potential has been probed in this comparison, although the collision energy has been rather low.

Missing measurements of HD-H2 means missing information for error estimates, but a lot of testing and even empirical improvement of the PES could be done in comparisons of measured and calculated H2-H2 data, as mentioned above. Additionally, the substitution of the HD molecule has been done carefully and at least tested once in the comparison with the crossed beam results. The determination of the important potential terms of HD-H2 is well understood; it is very similar to HD-He. Again, the (empirical) isotropic H2-H2 potential part determines mainly the isotropic (V_{000}) as well as the leading anisotropic term (V_{101}) of the HD-H2 interaction (Fig. 3). There is clearly no remaining uncertainty which could cause significant errors of the leading $\Delta j_{HD} = 1$ and - similar again to HD-He - the smaller $\Delta j_{HD} = 2$ cross sections and rate coefficients, as long as the angular momentum j_{H2} is kept fixed. From all this an upper error limit of 10% is assumed - due to the interaction potential - for the rate coefficients up to 300 K.

The cross sections and rate coefficients for the transfer of angular momentum between HD and H2 are rather delicate and inaccurate under several aspects. We realize at the first glance very small interaction potential terms in Figure 3 that could be responsible for a direct transition of this type, with the exception of V_{224}, but this one can contribute only to even Δj_{HD}, Δj_{H2} transitions which are rather exceptional because of the dominating $\Delta j_{HD} = 1$ transitions. The other potential terms are indeed very small and short in range such that any extended potential expansion of H2-H2 in the short c.m. distance range could provide major changes of these terms and subsequently large relative changes of the cross sections, especially at small collision energies. An important dynamical effect of subsequent excitation and de-excitation governed by the dominating anisotropies seems to provide increasing cross sections at the larger collision energies. The uncertainties of these cross sections and low temperature rate coefficients are of the order of a factor two, only due to the interaction potential. Additional errors, of all cross sections and rate coefficients mentioned so far, will be discussed in the next section.

3. Collision calculations and results.

Most of the integral cross sections and rate coefficients of HD-He are byproducts of a previous study (Köhler *et al.*, 1983a) of transport and orientation phenomena (Senftleben-Beenakker effects) for HD infinitely dilute in He gas. In preparation of this work partial wave expansions of scattering matrices had been obtained in close coupled collision calculations for initial angular momenta j_i of HD, $j_i = 0,1,2,3,4$, and 5, usually at more than 60 energy points. The rotational basis function sets used in the close coupled differential equation systems included all j's from 0 to j_i and the next two higher ones, with the exception of $j_i = 5$ where the $j = 7$ basis function has been skipped (we have therefore left out these results in the tables). A few partial wave expansions at higher energies have been added later on for each j_i in order to provide converged energy averaging of the rate coefficients up to $T = 600$ K. The maximum relative velocity point at 14000.0 m/s and $J_{max} = 125$ for its partial wave expansion have been found sufficient for this purpose. A selection of integral de-excitation cross sections is listed in Table 1, de-excitation and - for convenience - excitation rate coefficients are listed in Tables 2 and 3, respectively.

A summary of all calculated cross sections is shown graphically in Figure 4. The potential expansion shown in Figure 1 and the close coupled formalism (see e.g. Lester *et al.*, 1973) provide hints for a rough understanding of the findings. Every cross section curve starts up with a bump which is due to one or a few $l = 1$ orbiting resonances of the initial (j') state of the colliding system. The order in magnitude of the de-excitation cross sections at very small relative velocities is generally determined by the probabilities of just one direct and/or maybe two successive rotational transitions in the duration of one or a few total angular momentum (partial wave) collisions. The ordering maintained at large relative velocities is still determined partly by these simple transitions, but we should explain this phenomenon better as being due to ordered balances of successive up and down transitions which are represented in the partial wave expansion of a plane wave.

We may note that the cross section curves shown in Figure 4 as well as the listed data in Tables 1-3 have been calculated by using basis sets as described above. Extending of the basis by including higher rotational states, above $j' + 2$, causes in general *lowering* of the cross sections at large relative velocities. These corrections have been determined for excitation cross sections $\sigma_{0\to j}$ at two energy points, where the extended basis included $j_{max} = 8$. Results are shown in Figure 5. A general decrease of about 10% can be seen at large enough energies beyond the excitation thresholds of the additional rotational states. E.g., we see only a small correction of the $\sigma_{0\to 4}$ cross section at 6000 K, although transitions to $j = 7$ and 8 are classically allowed, while the correction can be considered almost saturated at 11000 K.

We estimate the consequences of our findings for the listed de-excitation cross sections of Table 1 and the rate coefficients $k_{j'\to j}$. Significant corrections start up at different relative kinetic energies depending upon the initial j' state: $j = 4$ becomes classically accessible for $j' = 1$ at about 1141 K and $j = 7$ becomes classically accessible for $j' = 4$ at about 2219 K. Compared to $k_{4\to 3}$, the noticeable corrections of $k_{1\to 0}$ start up at lower temperature. The corrections are small (< 10%) below room temperature: the integrand of the rate coefficient $k_{1\to 0}$ at 300 K temperature reaches the relative maximum at about 390 K, decreases to half maximum size at 910 K and has a long tail up to about

3800 K (10^{-4} of the maximum), while the integrand of $k_{4\to3}$ at 300 K temperature has the relative maximum at about 597 K, decreases to half maximum size at 1090 K and has a long tail up to about 4300 K. Thus noticeable corrections start up generally in the far out tail of the integrands and can provide changes to the rate coefficients of the order of 1%. Since we have no accurate experimental data for testing, especially for the leading inelastic cross sections and rate coefficients, the significance of the basis set corrections remains uncertain.

Possible corrections of rate coefficients above 300 K can also be expected from improvements of the interaction potential at short range - the V_4 term of the H2-He interaction needs improvement there - and vibrationally inelastic collisions which have been assumed being very small in this work. These unknown corrections increase certainly with increasing temperature and additionally, as mentioned in the previous section, more initial states of the higher rotational quantum numbers and probably vibrationally excited states contribute certainly to effective cross sections above 300 K.

Relative computational errors of the much smaller $\Delta j = 2, 3$, etc. cross sections and rate coefficients should be estimated larger than for $\Delta j = 1$, and they can be expected to increase with decreasing magnitude of the cross sections due to the numerical methods used for determining the scattering matrices. There is neither experimental evidence available indicating a need of improvement nor a serious theoretical estimate of the errors of these quantities.

Minor errors should also be mentioned which are included in all the results listed in Tables 1-3 and which, compared to the converged basis set, are about an order of magnitude less significant, e.g., the tolerances used in the calculations of the scattering matrices for determining the finite step sizes in the numerical integration procedures of the coupled differential equation systems, or the mesh of the PES grid determining slightly the interpolated elements of the potential matrices and their derivatives at fixed center of mass distances.

The calculations of rotational de-excitation cross sections and rate coefficients of HD in collision with H2 molecules have been performed in a somewhat improved manner, for economical reasons, but nevertheless converged results with respect to the basis function sets have been achieved. This will be explained now in detail for the HD - para-H2 system. The large basis sets used for testing the convergence of results obtained in less extended calculations are:

	(j_{HD}, j_{H2})
I :	(0,0) (1,0) (2,0) (3,0) (4,0) (0,2) (1,2) (2,2)
II :	(0,0) (1,0) (2,0) (3,0) (0,2) (1,2) (2,2) (3,2).

Integral cross sections for the j_{HD}, $j_{H2} = 1,0 \to 0,0$ transition have been calculated at 73 velocities, between 10.m/s and 6600.m/s (3160 K), by using a basis including (j_{HD}, j_{H2}) : (0,0), (1,0), (2,0), (3,0), (0,2), (1,2). The "orbiting" resonance features at small velocities have been perfectly displayed, starting with a sharp $l = 2$ peak which is followed by a broader $l = 3$ bump and an $l = 4$ shoulder. Tests of convergence at 2341., 3710., 4876., and 6286.m/s with the basis (I) and at 4154. and 6559.m/s with the basis (II) gave full (graphical) agreement as shown in Figure 6. A set of selected cross sections is listed in Table 4, rate coefficients for temperatures up to 300 K in Tables 5 and 6.

Integral cross sections for transitions from the initial angular momentum pair (0,2) to (0,0) as well as to (1,0) and (2,0) have been calculated by using the basis (j_{HD}, j_{H2}) : (0,0), (1,0), (2,0) (0,2), (1,2), (2,2) at 60 velocities. Results of convergence tests are shown in Figure 6, at 482., 2918., 4304., and 5854.m/s obtained from basis (I), and at 1791., 3465., and 6145.m/s obtained from basis (II). Full agreement has been found for $\sigma_{0,2\to0,0}$ up to 6000.m/s (and a small deviation at 6145.m/s which is negligible for the rate coefficients). Satisfying agreement has been achieved for $\sigma_{0,2\to1,0}$, and corrections of about 20-35% have been found for $\sigma_{0,2\to2,0}$ which decrease(!) at large velocities. The calculated cross sections of the three transitions are listed in Table 4. The two angular momentum transfer cross sections can have larger errors due to possible interaction potential changes as mentioned above. We may expect also larger than 10% computational errors because the absolute values of the cross section are much smaller than the leading ones - by more than a factor 40 at small velocities and roughly a factor 20 at the larger velocities.

There is a special connection between the $\sigma_{0,2\to0,0}$ cross sections of HD-H2 and H2-H2 which we should briefly discuss here because the results of the latter system determine the critically tested "two-state approximation" of the relaxation cross section and gave errors of the order of 10% at about 100 K temperature as shown in Figure 2. It is also interesting from the theoretical point of view that both cross sections are derived from the same electronic PES. The interaction potential terms (Fig. 3) governing the elastic scattering and the direct inelastic transitions, (V_{000} and V_{022}), are essentially the same for both systems, but the reduced masses are different (2203.05 and 1836.12 a.u.). The differences of the orbiting resonance features are therefore mainly due to the different masses and symmetries. The comparison is shown in Figure 7. Above the resonance features, starting at about 700.m/s and ranging up to about 2400.m/s, we find essentially the same cross sections. Then the H2-H2 cross section increases faster and prevails over the HD-H2 cross section at 6000.m/s by about 50%. The increasing difference is obviously due to the relatively strong forces acting on the HD molecule which provide the increase of $\sigma_{0,2\to1,0}$ and $\sigma_{0,2\to2,0}$ - on the cost of $\sigma_{0,2\to0,0}$.

The testing basis (I) has been used for obtaining cross sections $\sigma_{2,0\to0,0}$ and $\sigma_{2,0\to1,0}$ at nine velocities (Tab. 4). Since all de-excitation cross section curves are very similar, the $\sigma_{1,0\to0,0}$ curve has been used for interpolations between the nine points, by applying linear scaling between calculated pairs of $\sigma_{2,0\to0,0}$ and $\sigma_{2,0\to1,0}$. The result of this

procedure is shown in Figure 8 for $\sigma_{2,0\to0,0}$. Interpolated cross sections are included in Table 4. We should expect a small (lowering) correction of these cross sections at large velocities due to the neglect of $j_{HD} = 5$ in the basis. However, this means a very small correction of the rate coefficients because $j_{HD} = 5$ becomes classically accessible at roughly 4560.m/s and the corrections are in the far tails of the Maxwell-Boltzmann distribution functions. The estimated errors due to the applied interpolations are about 10% .

Furthermore, the testing basis set (II) has been used in calculations of $\sigma_{1,2\to0,2}$, $\sigma_{1,2\to0,0}$, $\sigma_{1,2\to1,0}$, and $\sigma_{1,2\to2,0}$ at five initial relative velocities. These four series of cross sections have also been interpolated, in the same way as just described. Some general findings should be noted: $\sigma_{1,2\to0,2}$ is comparable in magnitude to $\sigma_{1,0\to0,0}$, but larger at all relative velocities by a few per cent because more anisotropic interaction potential terms contribute to the dynamics when the H2 molecule rotates. The interpolation by using the $\sigma_{1,0\to0,0}$ grid gives small (<10%) errors. We may also expect a small (lowering) correction due to the neglect of $j_{H2} = 4$ in the basis, but only for the largest velocities. The calculated cross section of this transition may be assumed almost converged, except at 6000.m/s. The same holds obviously for $\sigma_{1,2\to0,0}$ which is comparable in size with $\sigma_{0,2\to1,0}$ up to 500.m/s initial relative velocity and becomes the smallest cross section in our list (Tab. 4) at 6000.m/s. The errors included by using one of our cross section grids for interpolations can be rather large at small relative velocities (≈ 50%) which holds also for the corresponding rate coefficients up to 100 K. The $\sigma_{1,2\to1,0}$ cross section is generally larger than $\sigma_{0,2\to0,0}$ because extra potential terms with an even first index (as V_{224}) contribute to the direct transitions. These cross sections are also reasonably converged with regard to the basis and the errors at small velocities due to interpolations (by using $\sigma_{0,2\to0,0}$) are small (≈ 20%). The last cross section out of this set of scattering matrices, $\sigma_{1,2\to2,0}$, is certainly not converged with respect to the basis. The angular momentum pairs (4,0) and (4,2) are neglected which could at best contribute two partly compensating corrections, but the errors could also be large (±40–50%), especially at large velocities. The errors of the rate coefficients below 100 K due to the applied interpolations can be rather large (≈ 50%) as well.

The cross sections and rate coefficients of the HD - ortho-H2 system have been determined from several basis function sets, while the testing was done with the sets

		(j_{HD}, j_{H2})
III	:	(0,1), (1,1), (2,1), (3,1), (0,3), (1,3), (2,3), (3,3)
IV	:	(0,1), (1,1), (2,1), (3,1), (4,1).

The de-excitation cross sections $\sigma_{1,1\to0,1}$ have been calculated at 66 velocity points with basis functions (0,1), (1,1), (2,1), and (3,1). Tests with the basis (III) gave small differences: less than 1% up to 4676.m/s, 1.3% at 6000.m/s and 3.6% at 6900.m/s. These corrections are included in the data listed in Table 7. The cross section curve, scaled according to the corrections, is shown in Figure 9. Tests results at large velocities derived from the basis (IV) show agreement with the listed data (< 1% corrections), i.e., about twice the amount of corrections as obtained from basis (III) can be expected from a basis set combining (III) and (IV). The listed integral cross sections up to about 5000.m/s and the rate coefficients (Tabs. 8 and 9) up to 100 K are practically converged, rate coefficients up to 300 K should have very small corrections due to the basis. The $\sigma_{1,1\to0,1}$ and $\sigma_{1,2\to0,2}$ cross sections and the corresponding rate coefficients are pretty much the same and both are slightly larger than $\sigma_{1,0\to0,0}$ because the same only small additional anisotropic potential terms produce little increase on the former ones.

Basis (III) has been used for calculations of cross sections $\sigma_{0,3\to0,1}$, $\sigma_{0,3\to1,1}$, and $\sigma_{0,3\to2,1}$ at seven velocities, and a reduced basis (without the angular momentum pairs (3,1) and (3,3)) gave almost converged results for $\sigma_{0,3\to0,1}$ and $\sigma_{0,3\to1,1}$ at 100., 450., 1200., 1500., and 3200.m/s. Useful cross section grids have been prepared by using the $\sigma_{1,1\to0,1}$ curve for interpolations. The very low temperature rate coefficients can include larger errors due to a lack of calculated cross sections in the resonance region, but in general we may consider the convergence and the estimate of errors of the three cross sections (listed in Tab. 7) and rate coefficients (listed in Tabs. 8 and 9) being practically the same as for the (0,2) → (j_1, j_2) transitions discussed baove. The same can be said about the four cross sections $\sigma_{1,3\to0,3}$, $\sigma_{1,3\to1,1}$, $\sigma_{1,3\to0,1}$ and $\sigma_{1,3\to2,1}$ and the corresponding rate coefficients, obtained by using basis (III), and compared with the (1,2) → (j_1, j_2) transitions, where again the last one cannot be converged with regard to the basis.

Since we know already from tests with the basis (IV) that inclusion of the $j_{H2} = 3$ state in the basis provides small corrections for pure j_{HD} transition cross sections, even at larger velocities, we can be optimistic about the quality of the fifteen points of $\sigma_{2,1\to1,1}$ and $\sigma_{2,1\to0,1}$ calculated by using basis (IV) and interpolated by scaling $\sigma_{1,1\to0,1}$. The cross section curves are shown in Figure 10. The upper one is leading in magnitude among others and is pretty much the same as $\sigma_{2,0\to1,0}$. We may expect again incomplete convergence of the cross sections at the largest velocities due to the neglect of $j_{H2} = 3$ and $j_{HD} = 5$ in the basis set, of the order of roughly 10% , while the rate coefficients (up to 300 K) should be essentially converged.

4. Similarities of the HD-He and the HD-H2 results.

The interaction potentials of HD-He and HD-H2 are similar under some aspects and we should take the opportunity to discuss possibilities of data exchange between or at least

common features of the two systems HD-He and HD-H2 - in view of rotationally inelastic dynamics.

We compare again potentials at fixed $r_{H2} = r_{HD} = 1.449$ a.u. and note that comparable potential terms shown in Figures 1 and 3 are the $V_\lambda(R)$ of Figure 1 divided by a factor $(2\lambda + 1)$ and the $V_{k0k}(R)/(4\pi)^{3/2}$, $(k = \lambda)$, as plotted in Figure 3. The zeros of the two isotropic interaction potentials differ by less than one tenth of an atomic unit, but V_{000} increases much steeper than V_0, with roughly a factor two over the entire repulsive potential range. The latter fact alone could provide significant differences of the cross sections. However, the same kind of substitution of H2 by HD molecules has been applied to the two PES which gave the leading anisotropic terms, V_{101} and V_1, among others for the substituted systems, terms which are roughly proportional to the derivative of the corresponding isotropic potential *versus* the center of mass distance R. This proportionality is important because it establishes almost the same *relative* leading anisotropies for the two interaction potentials: they differ by 13.4±2.6% between $3.0 \leq R \leq 5.2$ a.u. A comparison of some calculated results and a few test calculations give an answer to the question how much similarity follows for the cross sections. Figures 11a and b show the comparison of two $\Delta j_{HD} = 1$ de-excitation cross sections vs. relative velocity, $\sigma_{1,0\to0,0}$ with $\sigma_{1\to0}$, and $\sigma_{2,0\to1,0}$ with $\sigma_{2\to1}$. Changes of the HD-H2 potential by 1) scaling with a factor 0.5 (in order to remove the steeper increase of V_{000} but maintain the leading relative anisotropy) gave generally not very much smaller results (< 20% decrease) and 2), the additional replacement of the H2 by the He mass gave about the original cross sections again while the relative maximum was moved towards the HD-He cross section maximum. Since the same mass factor occurs when we draw the cross sections vs. relative kinetic energy, we can show the more obvious similarities of cross section curves in Figures 12a and b, especially at the larger collision energies.

We should firstly realize a remarkable consequence of the agreement found in the comparison of the two pairs of cross sections. When we now remember the leading-de-excitation cross sections of HD-He shown in Figure 4, the expectation of saturated $\Delta j_{HD} = 1$ de-excitation cross sections for the HD-H2 system, at larger relative velocities, seems to be rather obvious. One could also think in the next step of using some of the leading cross section curves of HD-He for HD-H2, without doing any collision calculation, but simply replacing the reduced mass in the rate coefficients. Perhaps this has been done already in the past. Another plausible estimate could be made by assuming that the next higher $\Delta j_{HD} = 1$ de-excitation cross sections, $\sigma_{3,j_2\to2,j_2}$ etc., and the corresponding rate coefficients are identical with $\sigma_{2,0\to1,0}$ and $k_{2,0\to1,0}$, while the excitation cross sections and rate coefficients could be derived by using the proper detailed balance formula. We will find out immediately that the last estimate is the best we can do.

Secondly we should realize the relation between the strong potential variations leading to the test results of Figure 11 and the rather small variations of the cross sections. E.g., scaling of the V_{101} term alone by a factor 0.9 could cause roughly the same amount of decrease of the two cross sections as the scaling by 0.5 of the full potential. The "scaling" of the reduced mass includes also a rather large factor (1.4243). Both variations conserve the relative anisotropies of the HD-H2 system exactly and they produce roughly a variation from the repulsive isotropic potential V_{000} and the leading anisotropy term V_{101} of HD-H2 to the repulsive isotropic potential V_0 and V_1 of HD-He. Smaller cross sections depending significantly upon other (smaller) anisotropic potential terms do not show these similarities.

Exactly the same cross sections of HD-H2 and HD-He (vs. energy) would give larger HD-H2 de-excitation rate coefficients: the factor

$$(\mu_{HD-He}/\mu_{HD-H2})^{1/2} = 1.1934$$

is obtained from the defining formula. Our calculated ratios $k_{2,0\to1,0}/k_{2\to1}$ are instead 1.592 at 100 K, 1.351 at 200 K, and 1.286 at 300 K. The calculated ratios for $k_{1,0\to0,0}/k_{1\to0}$ are in better agreement: 1.384 at 100 K, 1.284 at 200 K, and 1.277 at 300 K. The reason for the large deviations at 100 K (and even larger ones at lower temperatures) are low collision energy cross sections drawn in Figures 13a and b. The similarities are rather poor at this low collision energy range where the cross sections are very much determined by the masses of the two systems, the attractive interaction potential range, and only a small part of the repulsive potential nearby. The energy range sampled in Figure 13 includes the energies where the rate coefficient integrands reach their maximum, up to temperatures of about 100 K. The use of HD-He cross sections or rate coefficients for estimating cross sections or rate coefficients of HD-H2 is therefore not recommendable in these critical energy and temperature ranges.

5. Conclusions.

The cross sections and rate coefficients of transitions between a few of the lowest molecular rotational states of HD and H2 have been calculated for the collision systems HD-He and HD-H2, over relative velocity grids that turned out to be sufficient for obtaining rate coefficients of the HD-He system up to 600 K and of the HD-H2 system up to 300 K temperature. The set of the listed integral cross sections and rate coefficients allows to calculate converged effective (temperature dependent) cross sections of HD-He up to about 300 K temperature, and of HD-H2 up to about 100 K temperature. We have shown that, up to the latter temperatures, all the listed rate coefficients of HD-He and almost all the listed rate coefficients of HD-H2 can be con-

sidered converged to within a few per cent with respect to the basis functions.

Additional inaccuracies are due to the used potential energy surfaces, but there is not very much known about these shortcomings. The available measurements for HD-He which are containing integral cross sections or rate coefficients by definition could be used only for the probing of the dominating rate coefficients because of experimental uncertainties and, the few measured results do not cover the required ranges of energy and temperature listed in the tables. Observed quantities for HD-H2 which are defined by integral cross sections or rate coefficients are not available. Therefore, estimates of errors still included in the listed data have been tried by taking into account all the findings of comparisons of accurately calculated quantities - derived from the electronic potential energy surfaces used in this work - and measurements. Previous experience could be used from tests of the H2-He and H2-H2 systems. Since the isotropic potentials of both of these systems have been tested successfully many times, and even the leading anisotropic potential terms of both systems did very well in sensitive tests, we may assume $\approx 10\%$ errors for the leading $\Delta j_{HD} = 1$ and roughly twice as much for the $\Delta j_{HD} = 2$ cross sections and rate coefficients up to 300 K - when the angular momentum of H2 in HD-H2 is kept fixed. The angular momentum transfer cross sections and rate coefficients of HD-H2 are indeed small and much less accurately known, due to uncertainties of the interaction potential at small center of mass distances.

Estimates of the not yet calculated next higher $\Delta j_{HD} = 1$ de-excitation rate coefficients of HD-H2 are likely close to $k_{2,j_2 \to 1,j_2}$, whereas reasonable scaling of the corresponding rate coefficients of HD-He cannot be recommended because of major differences of the low relative kinetic energy cross sections.

References

Arthurs A.M., Dalgarno A.: 1960, *Proc. R. Soc. A* **256**, 540.

Buck U., Huisken F., Schleusener J., Schaefer J.: 1981, *J. Chem. Phys.* **74**, 535.

Buck U., Huisken F., Maneke G., Schaefer J.: 1983, *J. Chem. Phys.* **78**, 4430.

Buck U., Huisken F., Kohlhase A., Otten D., Schaefer J.: 1983, *J. Chem. Phys.* **78**, 4439.

Chu S.-I.: 1975, *J. Chem. Phys.* **62**, 4089.

Dilling W., Schaefer J.: 1989, *Z.f. Phys.* **13**, 207. Two shortcomings should be mentioned which seem to be due to experimental difficulties. One measured rotational relaxation cross section of para-H2-He discussed by Schaefer *et al.* (1985) is seriously different. And secondly, the measured low temperature second virial coefficients of the same system are very much different compared to theoretical results.

Farrar J.M., Lee Y.T.: 1972, *J. Chem. Phys.* **57**, 5492.

Gentry W.R., Giese C.F.: 1977, *J. Chem. Phys.* **67**, 5389.

Green S.: 1974, *Physica* **76**, 609.

Hermans P.W., Hermans L.J.F., Beenakker J.J.M.: 1983, *Physica* **122A**, 173.

Itikawa Y., Takayanagi K.: 1972, *J. Phys. Soc. Japan* **32**, 1605.

Jonkman R.M., Prangsma G.J., Ertas I., Knaap H.F.P., Beenakker J.J.M.: 1968, *Physica* **38**, 441.

Köhler W.E., Schaefer J.: 1983a, *Physica* **120A**, 185.

Köhler W.E., Schaefer J.: 1983b, *J. Chem. Phys.* **78**, 6602.

Lemaire C., Armstrong R.L., McCourt F.R.: 1984, *J. Chem. Phys.* **81**, 5275.

Lester Jr., W.A., Schaefer J.: 1973, *J. Chem. Phys.* **59**, 3676.

Meyer W., Hariharan P.C., Kutzelnigg W.: 1980, *J. Chem. Phys.* **73**, 1880.

Monchick L., Schaefer J.: 1987, *J. Chem. Phys.* **87**, 171.

Prangsma G.J., Heemskerk J.P.J., Knaap H.F.P., Beenakker J.J.M.: 1970, *Physica* **50**, 433.

Remark 1: These two independent sets of data have not been published.

Remark 2: Calculations are in progress for effective cross sections of para-H2 gas up to $T = 500$ K.

Schaefer J., Köhler W.E.: 1985, *Physica* **129A**, 469.

Schaefer J., Köhler W.E.: 1989, *Z.f.Phys.* **13**, 217.

Shafer R., Gordon R.G.: 1973, *J. Chem. Phys.* **58**, 542.

TABLE 1. *Rotational de-excitation cross sections of HD-He* ($j' \rightarrow j$) *in units of* 10^{-16} cm^2 vs. *relative center of mass velocities; (+2) :=* 10^{+2}.

v(m/s)	1 → 0	2 → 1	2 → 0	3 → 2	3 → 1
40.	3.70(+1)				
60.	4.35(+1)	3.58(+1)	3.24(+0)	1.97(+1)	1.93(+0)
80.	2.28(+1)				
100.	1.16(+1)	9.97(+0)	8.97(-1)	5.52(+0)	5.35(-1)
140.	5.72(+0)	4.88(+0)	4.37(-1)	2.68(+0)	2.59(-1)
180.	4.21(+0)	3.60(+0)	3.21(-1)	1.98(+0)	1.91(-1)
220.	3.05(+0)	2.61(+0)	2.33(-1)	1.44(+0)	1.39(-1)
260.	2.45(+0)	2.10(+0)	1.87(-1)	1.17(+0)	1.12(-1)
300.	2.10(+0)	1.80(+0)	1.60(-1)	1.00(+0)	9.62(-2)
360.	1.75(+0)	1.50(+0)	1.34(-1)	8.50(-1)	8.12(-2)
480.	1.43(+0)	1.23(+0)	1.11(-1)	7.18(-1)	6.86(-2)
560.	1.33(+0)	1.16(+0)	1.06(-1)	6.89(-1)	6.60(-2)
650.	1.28(+0)	1.13(+0)	1.04(-1)	6.86(-1)	6.60(-2)
850.	1.26(+0)	1.18(+0)	1.12(-1)	7.43(-1)	7.32(-2)
950.	1.28(+0)	1.24(+0)	1.20(-1)	7.93(-1)	7.96(-2)
1100.	1.33(+0)	1.35(+0)	1.35(-1)	8.89(-1)	9.21(-2)
1300.	1.43(+0)	1.53(+0)	1.60(-1)	1.05(+0)	1.14(-1)
1500.	1.55(+0)	1.73(+0)	1.90(-1)	1.24(+0)	1.43(-1)
1700.	1.64(+0)	1.94(+0)	2.23(-1)	1.45(+0)	1.79(-1)
1900.	1.73(+0)	2.15(+0)	2.60(-1)	1.68(+0)	2.22(-1)
2000.	1.77(+0)	2.25(+0)	2.77(-1)		
2400.	1.92(+0)	2.57(+0)	3.44(-1)	2.28(+0)	3.51(-1)
2800.	2.05(+0)	2.81(+0)	4.00(-1)	2.68(+0)	4.62(-1)
3200.	2.14(+0)	2.98(+0)	4.44(-1)	2.98(+0)	5.66(-1)
3600.	2.18(+0)	3.08(+0)	4.75(-1)	3.15(+0)	6.55(-1)
4000.	2.18(+0)	3.13(+0)	4.94(-1)	3.24(+0)	7.27(-1)
4400.	2.16(+0)	3.13(+0)	5.01(-1)	3.26(+0)	7.80(-1)
4800.	2.11(+0)	3.11(+0)	4.97(-1)		

v(m/s)	1 → 0	2 → 1	2 → 0	3 → 2	3 → 1
5200.	2.07(+0)	3.07(+0)	4.87(-1)	3.21(+0)	8.43(-1)
5600.	2.03(+0)	3.02(+0)	4.72(-1)		
6000.	2.00(+0)	2.96(+0)	4.56(-1)	3.11(+0)	8.60(-1)
6400.	1.97(+0)	2.90(+0)	4.40(-1)		
6800.	1.96(+0)	2.86(+0)	4.26(-1)	3.01(+0)	8.48(-1)
7300.		2.80(+0)	4.11(-1)		
7600.	1.94(+0)				
7900.		2.73(+0)	3.99(-1)	3.88(+0)	8.14(-1)
8200.	1.90(+0)				
8500.		2.66(+0)	3.91(-1)		
8800.	1.85(+0)				
9100.		2.59(+0)	3.85(-1)	3.73(+0)	7.76(-1)
9400.	1.79(+0)				
9700.		2.51(+0)	3.78(-1)		
10000.	1.72(+0)				
10300.		2.44(+0)	3.71(-1)	2.59(+0)	7.45(-1)
10600.	1.67(+0)				
11000.		2.36(+0)	3.62(-1)		
11400.	1.63(+0)				
11800.		2.30(+0)	3.55(-1)	2.49(+0)	7.07(-1)
12200.	1.61(+0)				
12600.		2.25(+0)	3.54(-1)		
13000.	1.61(+0)				
14000.	1.59(+0)	2.21(+0)	3.54(-1)	2.39(+0)	6.74(-1)

v(m/s)	3 → 0	4 → 3	4 → 2	4 → 1	4 → 0
60.	3.74(-1)				
100.	1.03(-1)				
140.	5.00(-2)	1.48(+0)	1.34(-1)	2.74(-2)	4.71(-3)
180.	3.67(-2)				
220.	2.67(-2)	7.93(-1)	7.12(-2)	1.46(-2)	2.50(-3)
260.	2.15(-2)				
300.	1.84(-2)	5.48(-1)	4.91(-2)	1.00(-2)	1.72(-3)
360.	1.56(-2)				
480.	1.31(-2)	3.87(-1)	3.48(-2)	7.13(-3)	1.22(-3)
560.	1.27(-2)	3.71(-1)	3.36(-2)	6.90(-3)	1.18(-3)
650.	1.27(-2)	3.71(-1)	3.39(-2)	6.99(-3)	1.19(-3)
850.	1.43(-2)	4.13(-1)	3.87(-2)	8.11(-3)	1.39(-3)
950.	1.56(-2)	4.49(-1)	4.28(-2)	9.07(-3)	1.55(-3)
1100.	1.83(-2)	5.19(-1)	5.11(-2)	1.10(-2)	1.89(-3)
1300.	2.33(-2)	6.40(-1)	6.59(-2)	1.46(-2)	2.52(-3)
1500.	2.99(-2)	7.88(-1)	8.57(-2)	1.95(-2)	3.40(-3)
1900.	4.88(-2)	1.16(+0)	1.43(-1)	3.48(-2)	6.26(-3)
2400.	8.34(-2)	1.73(+0)	2.52(-1)	6.78(-2)	1.28(-2)
2800.	1.17(-1)	2.21(+0)	3.66(-1)	1.06(-1)	2.11(-2)
3200.	1.53(-1)	2.63(+0)	4.89(-1)	1.54(-1)	3.22(-2)
3600.	1.89(-1)	2.94(+0)	6.07(-1)	2.09(-1)	4.58(-2)
4000.	2.23(-1)	3.14(+0)	7.09(-1)	2.65(-1)	6.15(-2)
4400.	2.52(-1)	3.23(+0)	7.92(-1)	3.20(-1)	7.84(-2)
5200.	2.92(-1)	3.23(+0)	8.97(-1)	4.13(-1)	1.12(-1)
6000.	3.05(-1)	3.13(+0)	9.42(-1)	4.74(-1)	1.40(-1)
6800.	2.99(-1)	3.02(+0)	9.51(-1)	5.03(-1)	1.58(-1)
7900.	2.80(-1)	2.89(+0)	9.38(-1)	5.06(-1)	1.65(-1)
9100.	2.61(-1)	2.75(+0)	9.07(-1)	4.87(-1)	1.60(-1)
10300.	2.44(-1)	2.64(+0)	8.67(-1)	4.60(-1)	1.54(-1)
11800.	2.25(-1)	2.56(+0)	8.22(-1)	4.35(-1)	1.46(-1)
14000.	2.07(-1)	2.47(+0)	7.82(-1)	4.13(-1)	1.35(-1)

TABLE 2. *De-excitation rate coefficients of HD-He* (cm^3/sec).

T(K)	1 → 0	2 → 1	2 → 0	3 → 2	3 → 1
10.	7.16(-12)	6.19(-12)	5.56(-13)	3.52(-12)	3.37(-13)
20.	7.73(-12)	6.86(-12)	6.28(-13)	4.05(-12)	3.92(-13)
30.	8.70(-12)	7.96(-12)	7.46(-13)	4.86(-12)	4.78(-13)
40.	9.78(-12)	9.21(-12)	8.84(-13)	5.79(-12)	5.83(-13)
60.	1.20(-11)	1.20(-11)	1.20(-12)	7.93(-12)	8.42(-13)
80.	1.43(-11)	1.49(-11)	1.56(-12)	1.03(-11)	1.15(-12)
100.	1.64(-11)	1.79(-11)	1.94(-12)	1.28(-11)	1.50(-12)
120.	1.86(-11)	2.09(-11)	2.34(-12)	1.53(-11)	1.88(-12)
140.	2.06(-11)	2.38(-11)	2.74(-12)	1.79(-11)	2.30(-12)
160.	2.26(-11)	2.66(-11)	3.14(-12)	2.06(-11)	2.74(-12)
180.	2.46(-11)	2.94(-11)	3.55(-12)	2.32(-11)	3.21(-12)
200.	2.64(-11)	3.22(-11)	3.95(-12)	2.60(-11)	3.70(-12)
220.	2.82(-11)	3.48(-11)	4.35(-12)	2.86(-11)	4.20(-12)
240.	3.00(-11)	3.74(-11)	4.75(-12)	3.13(-11)	4.72(-12)
260.	3.17(-11)	3.99(-11)	5.14(-12)	3.40(-11)	5.26(-12)
280.	3.34(-11)	4.24(-11)	5.53(-12)	3.66(-11)	5.80(-12)
300.	3.50(-11)	4.48(-11)	5.92(-12)	3.92(-11)	6.34(-12)
320.	3.65(-11)	4.71(-11)	6.29(-12)	4.18(-11)	6.89(-12)
340.	3.80(-11)	4.94(-11)	6.66(-12)	4.42(-11)	7.44(-12)
360.	3.95(-11)	5.16(-11)	7.02(-12)	4.67(-11)	7.98(-12)
380.	4.09(-11)	5.38(-11)	7.38(-12)	4.91(-11)	8.53(-12)
400.	4.23(-11)	5.59(-11)	7.72(-12)	5.14(-11)	9.08(-12)
440.	4.50(-11)	6.00(-11)	8.40(-12)	5.60(-11)	1.02(-11)
480.	4.75(-11)	6.38(-11)	9.04(-12)	6.03(-11)	1.12(-11)
520.	4.99(-11)	6.75(-11)	9.66(-12)	6.44(-11)	1.23(-11)
560.	5.22(-11)	7.10(-11)	1.02(-11)	6.83(-11)	1.33(-11)
600.	5.43(-11)	7.44(-11)	1.08(-11)	7.21(-11)	1.43(-11)

T(K)	3 → 0	4 → 3	4 → 2	4 → 1	4 → 0
10.	6.48(-14)	1.89(-12)	1.70(-13)	3.48(-14)	5.95(-15)
20.	7.55(-14)	2.19(-12)	1.99(-13)	4.12(-14)	7.03(-15)
30.	9.30(-14)	2.66(-12)	2.47(-13)	5.15(-14)	8.84(-15)
40.	1.15(-13)	3.23(-12)	3.08(-13)	6.54(-14)	1.12(-14)
60.	1.70(-13)	4.60(-12)	4.65(-13)	1.02(-13)	1.77(-14)
80.	2.38(-13)	6.18(-12)	6.59(-13)	1.49(-13)	2.62(-14)
100.	3.17(-13)	8.03(-12)	9.04(-13)	2.12(-13)	3.81(-14)
120.	4.07(-13)	9.77(-12)	1.17(-12)	2.85(-13)	5.18(-14)
140.	5.08(-13)	1.20(-11)	1.47(-12)	3.82(-13)	6.91(-14)
160.	6.18(-13)	1.42(-11)	1.80(-12)	4.71(-13)	8.95(-14)
180.	7.39(-13)	1.65(-11)	2.24(-12)	5.88(-13)	1.12(-13)
200.	8.67(-13)	1.90(-11)	2.64(-12)	7.09(-13)	1.41(-13)
220.	1.00(-12)	2.07(-11)	3.00(-12)	8.23(-13)	1.64(-13)
240.	1.14(-12)	2.30(-11)	3.46(-12)	9.68(-13)	1.97(-13)
260.	1.29(-12)	2.55(-11)	4.00(-12)	1.16(-12)	2.31(-13)
280.	1.45(-12)	2.80(-11)	4.38(-12)	1.29(-12)	2.68(-13)
300.	1.60(-12)	2.97(-11)	4.86(-12)	1.46(-12)	3.09(-13)
320.	1.76(-12)	3.16(-11)	5.34(-12)	1.63(-12)	3.49(-13)
340.	1.93(-12)	3.42(-11)	5.76(-12)	1.78(-12)	3.83(-13)
360.	2.09(-12)	3.75(-11)	6.45(-12)	2.06(-12)	4.39(-13)
380.	2.26(-12)	4.03(-11)	6.80(-12)	2.17(-12)	4.78(-13)
400.	2.43(-12)	4.26(-11)	7.50(-12)	2.47(-12)	5.34(-13)
440.	2.77(-12)	4.54(-11)	8.38(-12)	2.79(-12)	6.29(-13)
480.	3.11(-12)	5.09(-11)	9.63(-12)	3.28(-12)	7.47(-13)
520.	3.45(-12)	5.31(-11)	1.06(-11)	3.69(-12)	8.55(-13)
560.	3.79(-12)	5.82(-11)	1.16(-11)	4.14(-12)	9.75(-13)
600.	4.13(-12)	6.31(-11)	1.29(-11)	4.68(-12)	1.11(-12)

TABLE 3. *Excitation rate coefficients of HD-He* (cm^3/sec).

T(K)	0 → 1	0 → 2	1 → 2	0 → 3	1 → 3
10.	5.70(-17)	5.67(-28)	7.93(-23)	2.46(-47)	1.60(-41)
20.	3.78(-14)	1.42(-20)	3.17(-17)	1.23(-28)	1.30(-26)
30.	3.62(-13)	1.02(-17)	2.62(-15)	5.30(-24)	6.56(-22)
40.	1.18(-12)	2.97(-16)	2.56(-14)	3.87(-21)	1.62(-19)
60.	4.24(-12)	9.95(-15)	2.80(-13)	3.39(-18)	4.77(-17)
80.	8.59(-12)	6.41(-14)	1.02(-12)	1.16(-16)	9.29(-16)
100.	1.37(-11)	2.08(-13)	2.31(-12)	1.05(-15)	5.95(-15)
120.	1.91(-11)	4.75(-13)	4.12(-12)	4.81(-15)	2.16(-14)
140.	2.48(-11)	8.79(-13)	6.37(-12)	1.49(-14)	5.64(-14)
160.	3.04(-11)	1.42(-12)	8.97(-12)	3.61(-14)	1.19(-13)
180.	3.61(-11)	2.10(-12)	1.18(-11)	7.33(-14)	2.17(-13)
200.	4.17(-11)	2.89(-12)	1.49(-11)	1.32(-13)	3.56(-13)
220.	4.73(-11)	3.79(-12)	1.81(-11)	2.16(-13)	5.41(-13)
240.	5.27(-11)	4.79(-12)	2.15(-11)	3.30(-13)	7.74(-13)
260.	5.81(-11)	5.87(-12)	2.49(-11)	4.76(-13)	1.06(-12)
280.	6.33(-11)	7.01(-12)	2.83(-11)	6.56(-13)	1.39(-12)
300.	6.84(-11)	8.22(-12)	3.18(-11)	8.74(-13)	1.77(-12)
320.	7.33(-11)	9.47(-12)	3.53(-11)	1.13(-12)	2.19(-12)
340.	7.82(-11)	1.08(-11)	3.88(-11)	1.42(-12)	2.66(-12)
360.	8.29(-11)	1.21(-11)	4.23(-11)	1.74(-12)	3.17(-12)
380.	8.76(-11)	1.34(-11)	4.57(-11)	2.11(-12)	3.72(-12)
400.	9.20(-11)	1.48(-11)	4.91(-11)	2.50(-12)	4.30(-12)
440.	1.01(-09)	1.75(-11)	5.59(-11)	3.40(-12)	5.56(-12)
480.	1.09(-09)	2.03(-11)	6.24(-11)	4.42(-12)	6.94(-12)
520.	1.17(-09)	2.31(-11)	6.88(-11)	5.54(-12)	8.40(-12)
560.	1.24(-09)	2.58(-11)	7.49(-11)	6.76(-12)	9.93(-12)
600.	1.32(-09)	2.85(-11)	8.09(-11)	8.07(-12)	1.15(-11)

T(K)	2 → 3	0 → 4	1 → 4	2 → 4	3 → 4
10.	1.31(-28)	3.43(-70)	2.52(-64)	9.60(-53)	2.87(-35)
20.	2.92(-20)	1.60(-42)	1.92(-39)	2.01(-32)	3.06(-23)
30.	2.03(-17)	3.18(-32)	4.46(-30)	6.52(-26)	1.68(-19)
40.	5.82(-16)	1.63(-27)	7.74(-26)	1.31(-22)	1.37(-17)
60.	1.92(-14)	1.02(-22)	1.64(-21)	3.20(-19)	1.31(-15)
80.	1.22(-13)	3.04(-20)	2.81(-19)	1.82(-17)	1.44(-14)
100.	3.93(-13)	1.03(-18)	6.95(-18)	2.30(-16)	6.63(-14)
120.	8.90(-13)	1.17(-17)	6.20(-17)	1.30(-15)	1.87(-13)
140.	1.64(-12)	6.99(-17)	3.18(-16)	4.71(-15)	4.17(-13)
160.	2.65(-12)	2.80(-16)	1.12(-15)	1.27(-14)	7.77(-13)
180.	3.90(-12)	8.48(-16)	3.09(-15)	2.93(-14)	1.28(-12)
200.	5.39(-12)	2.12(-15)	7.03(-15)	5.65(-14)	1.95(-12)
220.	7.08(-12)	4.56(-15)	1.37(-14)	9.60(-14)	2.68(-12)
240.	8.94(-12)	8.77(-15)	2.48(-14)	1.55(-13)	3.61(-12)
260.	1.10(-11)	1.55(-14)	4.28(-14)	2.38(-13)	4.70(-12)
280.	1.31(-11)	2.54(-14)	6.54(-14)	3.32(-13)	5.92(-12)
300.	1.54(-11)	3.95(-14)	9.74(-14)	4.56(-13)	7.09(-12)
320.	1.77(-11)	5.84(-14)	1.38(-13)	6.02(-13)	8.39(-12)
340.	2.02(-11)	8.30(-14)	1.85(-13)	7.65(-13)	1.00(-11)
360.	2.26(-11)	1.14(-13)	2.58(-13)	9.89(-13)	1.19(-11)
380.	2.52(-11)	1.52(-13)	3.22(-13)	1.19(-12)	1.28(-11)
400.	2.77(-11)	1.99(-13)	4.27(-13)	1.47(-12)	1.53(-11)
440.	3.29(-11)	3.15(-13)	6.24(-13)	2.01(-12)	1.85(-11)
480.	3.81(-11)	4.76(-13)	9.10(-13)	2.73(-12)	2.29(-11)
520.	4.33(-11)	6.68(-13)	1.23(-12)	3.45(-12)	2.59(-11)
560.	4.84(-11)	9.07(-13)	1.62(-12)	4.30(-12)	3.03(-11)
600.	5.34(-11)	1.20(-12)	2.09(-12)	5.29(-12)	3.50(-11)

TABLE 4. *Rotational de-excitation cross sections of HD and para-H2* ($j_1' j_2' \rightarrow j_1 j_2$) *in units of* 10^{-16} cm^2vs. *relative center of mass velocities; *: calculated.*

v(m/s)	1,0 → 0,0	2,0 → 1,0	2,0 → 0,0	1,2 → 0,2	1,2 → 2,0
30.	*8.21(+1)	3.84(+1)	2.33(+0)	9.32(+1)	2.11(-1)
40.	*9.22(+1)	*4.32(+1)	*2.61(+0)	1.05(+2)	5.86(-1)
60.	*1.82(+2)	3.96(+2)	1.38(+1)	2.07(+2)	1.31(+0)
70.	*8.03(+1)	2.63(+2)	8.59(+0)	9.12(+1)	2.82(+0)
80.	*4.72(+1)	*2.15(+2)	*6.74(+0)	5.36(+1)	5.38(-1)
90.	*3.32(+1)	1.44(+2)	4.57(+0)	3.77(+1)	2.20(-1)
100.	*2.56(+1)	1.04(+2)	3.38(+0)	*2.90(+1)	*1.49(-1)
120.	*1.74(+1)	6.07(+1)	2.07(+0)	1.97(+1)	9.36(-2)
150.	*1.15(+1)	2.78(+1)	1.10(+0)	1.29(+1)	5.95(-2)
180.	*8.52(+0)	*9.45(+0)	*5.72(-1)	9.55(+0)	4.33(-2)
210.	*7.44(+0)	8.12(+0)	4.90(-1)	8.28(+0)	3.69(-2)
240.	*8.99(+0)	9.64(+0)	5.79(-1)	9.94(+0)	4.32(-2)
270.	*1.15(+1)	*1.20(+1)	*7.18(-1)	1.26(+1)	5.53(-2)
300.	*8.56(+0)	9.06(+0)	5.41(-1)	9.30(+0)	4.11(-2)
360.	*4.75(+0)	5.12(+0)	3.05(-1)	5.04(+0)	2.19(-2)
450.	*3.77(+0)	*4.20(+0)	*2.50(-1)	*3.83(+0)	*1.60(-2)
520.	*2.94(+0)	3.30(+0)	1.97(-1)	3.00(+0)	1.30(-2)
600.	*2.49(+0)	2.82(+0)	1.69(-1)	2.53(+0)	1.14(-2)
800.	*1.87(+0)	2.17(+0)	1.32(-1)	1.90(+0)	9.83(-3)
1200.	*1.52(+0)	1.88(+0)	1.18(-1)	*1.55(+0)	*1.24(-2)
1400.	*1.50(+0)	*1.95(+0)	*1.25(-1)	1.53(+0)	1.68(-2)
1800.	*1.59(+0)	2.06(+0)	1.42(-1)	1.62(+0)	2.40(-2)
2300.	*1.75(+0)	2.28(+0)	1.74(-1)	1.78(+0)	3.51(-2)
2900.	*2.01(+0)	2.62(+0)	2.31(-1)	2.04(+0)	5.85(-2)
3200.	*2.14(+0)	*2.78(+0)	*2.65(-1)	*2.16(+0)	*7.14(-2)
3600.	*2.29(+0)	2.96(+0)	3.08(-1)	2.33(+0)	8.89(-2)
4500.	*2.48(+0)	*3.15(+0)	*4.06(-1)	2.57(+0)	1.27(-1)
5000.	*2.51(+0)	3.22(+0)	4.56(-1)	2.62(+0)	1.43(-1)
5500.	*2.49(+0)	3.23(+0)	5.02(-1)	2.63(+0)	1.54(-1)
6000.	*2.44(+0)	*3.20(+0)	*5.44(-1)	*2.60(+0)	*1.60(-1)

v(m/s)	1,2 → 1,0	1,2 → 0,0	0,2 → 0,0	0,2 → 1,0	0,2 → 2,0
30.	1.67(+0)	2.98(-1)	*5.92(-1)	*1.38(-1)	*1.09(-2)
40.	1.88(+0)	3.35(-1)	*1.81(+0)	*3.84(-1)	*2.23(-2)
60.	3.72(+0)	6.63(-1)	*4.13(+0)	*8.59(-1)	*6.16(-2)
70.	1.64(+0)	2.92(-1)	*9.30(+0)	*1.85(+0)	*1.78(-1)
80.	9.63(-1)	1.72(-1)	*1.16(+0)	*3.53(-1)	*5.59(-2)
90.	6.76(-1)	1.21(-1)	*6.12(-1)	*1.44(-1)	*1.48(-2)
100.	*5.21(-1)	*9.29(-2)	*4.28(-1)	*9.76(-2)	*8.90(-3)
120.	3.54(-1)	6.29(-2)	*2.74(-1)	*6.16(-2)	*5.19(-3)
150.	2.33(-1)	4.14(-2)	*1.76(-1)	*3.95(-2)	*3.21(-3)
180.	1.72(-1)	3.05(-2)	*1.30(-1)	*2.91(-2)	*2.33(-3)
210.	1.50(-1)	2.64(-2)	*1.13(-1)	*2.51(-2)	*1.99(-3)
240.	1.80(-1)	3.16(-2)	*1.38(-1)	*2.98(-2)	*2.32(-3)

TABLE 4. *(Continued)*

270.	2.29(-1)	3.99(-2)	*1.81(-1)	*3.88(-2)	*3.01(-3)
300.	1.70(-1)	2.95(-2)	*1.36(-1)	*2.94(-2)	*2.31(-3)
360.	9.31(-2)	1.59(-2)	*7.49(-2)	*1.64(-2)	*1.30(-3)
450.	*7.20(-2)	*1.20(-2)	*6.04(-2)	*1.32(-2)	*1.04(-3)
520.	5.75(-2)	9.51(-3)	*4.82(-2)	*1.06(-2)	*8.39(-4)
600.	4.99(-2)	8.22(-3)	*4.17(-2)	*9.28(-3)	*7.33(-4)
800.	4.05(-2)	6.60(-3)	*3.36(-2)	*7.84(-3)	*6.21(-4)
1200.	*4.00(-2)	*6.35(-3)	*3.19(-2)	*9.36(-3)	*7.33(-4)
1400.	4.05(-2)	6.81(-3)	*3.17(-2)	*1.27(-2)	*1.03(-3)
1800.	4.50(-2)	8.50(-3)	*3.54(-2)	*1.80(-2)	*1.71(-3)
2300.	5.34(-2)	1.17(-2)	4.16(-2)	2.81(-2)	4.40(-3)
2900.	6.79(-2)	1.75(-2)	*4.92(-2)	*4.31(-2)	*9.69(-3)
3200.	*7.62(-2)	2.10(-2)	*5.26(-2)	*5.23(-2)	*1.40(-2)
3600.	8.30(-2)	2.57(-2)	*5.66(-2)	*6.52(-2)	*2.16(-2)
4500.	9.42(-2)	3.70(-2)	*6.49(-2)	*9.38(-2)	*4.81(-2)
5000.	9.80(-2)	4.35(-2)	*7.00(-2)	*1.06(-1)	*6.91(-2)
5500.	1.00(-1)	4.97(-2)	*7.62(-2)	*1.15(-1)	*9.47(-2)
6000.	*1.01(-1)	*5.57(-2)	*8.40(-2)	*1.20(-1)	*1.25(-1)

TABLE 5. *Rotational de-excitation rate coefficients of HD and para-H2* ($j_1' j_2' \rightarrow j_1 j_2$) *in* $cm^3 sec^{-1}$ *units.*

T(K)	1,0 → 0,0	2,0 → 1,0	2,0 → 0,0	1,2 → 0,2	1,2 → 2,0
10.	1.85(-11)	2.32(-11)	1.27(-12)	1.97(-11)	9.32(-14)
20.	1.69(-11)	2.01(-11)	1.17(-12)	1.76(-11)	8.62(-14)
30.	1.67(-11)	1.99(-11)	1.18(-12)	1.72(-11)	9.53(-14)
40.	1.71(-11)	2.05(-11)	1.25(-12)	1.76(-11)	1.12(-13)
50.	1.78(-11)	2.16(-11)	1.34(-12)	1.83(-11)	1.35(-13)
60.	1.87(-11)	2.28(-11)	1.44(-12)	1.91(-11)	1.61(-13)
70.	1.96(-11)	2.42(-11)	1.55(-12)	2.00(-11)	1.89(-13)
80.	2.06(-11)	2.56(-11)	1.67(-12)	2.10(-11)	2.19(-13)
90.	2.16(-11)	2.70(-11)	1.80(-12)	2.20(-11)	2.51(-13)
100.	2.27(-11)	2.85(-11)	1.92(-12)	2.31(-11)	2.86(-13)
110.	2.38(-11)	3.00(-11)	2.06(-12)	2.42(-11)	3.22(-13)
120.	2.49(-11)	3.15(-11)	2.20(-12)	2.53(-11)	3.61(-13)
130.	2.60(-11)	3.30(-11)	2.34(-12)	2.65(-11)	4.02(-13)
140.	2.71(-11)	3.45(-11)	2.49(-12)	2.76(-11)	4.45(-13)
150.	2.82(-11)	3.60(-11)	2.64(-12)	2.87(-11)	4.89(-13)
160.	2.94(-11)	3.75(-11)	2.80(-12)	2.99(-11)	5.34(-13)
170.	3.05(-11)	3.90(-11)	2.96(-12)	3.10(-11)	5.82(-13)
180.	3.16(-11)	4.05(-11)	3.12(-12)	3.22(-11)	6.30(-13)
190.	3.27(-11)	4.20(-11)	3.28(-12)	3.33(-11)	6.80(-13)
200.	3.39(-11)	4.35(-11)	3.44(-12)	3.45(-11)	7.31(-13)
220.	3.61(-11)	4.64(-11)	3.78(-12)	3.67(-11)	8.35(-13)
240.	3.83(-11)	4.93(-11)	4.12(-12)	3.90(-11)	9.43(-13)
260.	4.04(-11)	5.21(-11)	4.47(-12)	4.12(-11)	1.05(-12)
280.	4.26(-11)	5.48(-11)	4.82(-12)	4.34(-11)	1.17(-12)
300.	4.47(-11)	5.76(-11)	5.18(-12)	4.55(-11)	1.28(-12)

T(K)	1,2 → 1,0	1,2 → 0,0	0,2 → 2,0	0,2 → 1,0	0,2 → 0,0
10.	3.69(-13)	6.28(-14)	7.21(-15)	6.93(-14)	3.14(-13)
20.	3.49(-13)	5.82(-14)	6.72(-15)	6.64(-14)	2.90(-13)
30.	3.63(-13)	6.01(-14)	7.40(-15)	7.34(-14)	2.98(-13)
40.	3.89(-13)	6.46(-14)	8.84(-15)	8.58(-14)	3.17(-13)
50.	4.21(-13)	7.06(-14)	1.09(-14)	1.02(-13)	3.40(-13)
60.	4.55(-13)	7.76(-14)	1.36(-14)	1.20(-13)	3.66(-13)
70.	4.91(-13)	8.54(-14)	1.70(-14)	1.40(-13)	3.93(-13)
80.	5.28(-13)	9.40(-14)	2.11(-14)	1.62(-13)	4.21(-13)
90.	5.67(-13)	1.03(-13)	2.61(-14)	1.84(-13)	4.49(-13)
100.	6.06(-13)	1.13(-13)	3.21(-14)	2.09(-13)	4.77(-13)
110.	6.47(-13)	1.23(-13)	3.90(-14)	2.35(-13)	5.06(-13)
120.	6.88(-13)	1.34(-13)	4.69(-14)	2.62(-13)	5.34(-13)
130.	7.29(-13)	1.46(-13)	5.58(-14)	2.91(-13)	5.64(-13)
140.	7.71(-13)	1.58(-13)	6.56(-14)	3.21(-13)	5.94(-13)
150.	8.14(-13)	1.70(-13)	7.63(-14)	3.52(-13)	6.23(-13)
160.	8.57(-13)	1.83(-13)	8.80(-14)	3.85(-13)	6.53(-13)
170.	9.00(-13)	1.96(-13)	1.01(-13)	4.18(-13)	6.83(-13)
180.	9.44(-13)	2.09(-13)	1.14(-13)	4.52(-13)	7.14(-13)
190.	9.87(-13)	2.23(-13)	1.29(-13)	4.88(-13)	7.44(-13)
200.	1.03(-12)	2.37(-13)	1.44(-13)	5.24(-13)	7.73(-13)
220.	1.12(-12)	2.67(-13)	1.78(-13)	5.98(-13)	8.33(-13)
240.	1.20(-12)	2.97(-13)	2.14(-13)	6.75(-13)	8.92(-13)
260.	1.29(-12)	3.28(-13)	2.55(-13)	7.54(-13)	9.51(-13)
280.	1.38(-12)	3.61(-13)	2.99(-13)	8.34(-13)	1.01(-12)
300.	1.46(-12)	3.94(-13)	3.46(-13)	9.17(-13)	1.07(-12)

TABLE 6. *Rotational excitation rate coefficients of HD and para-H2* ($j_1' j_2' \rightarrow j_1 j_2$) *in* $cm^3 sec^{-1}$ *units.*

T(K)	0,0 → 1,0	1,0 → 2,0	0,0 → 2,0	0,2 → 1,2	2,0 → 1,2
10.	1.47(-16)	2.97(-22)	1.29(-28)	1.56(-16)	2.61(-24)
20.	8.25(-14)	9.27(-17)	2.63(-20)	8.58(-14)	7.90(-19)
30.	6.95(-13)	6.53(-15)	1.62(-17)	7.16(-13)	6.02(-17)
40.	2.08(-12)	5.70(-14)	4.20(-16)	2.13(-12)	5.90(-16)
50.	4.10(-12)	2.16(-13)	3.07(-15)	4.20(-12)	2.52(-15)
60.	6.59(-12)	5.35(-13)	1.19(-14)	6.74(-12)	6.99(-15)
70.	9.39(-12)	1.04(-12)	3.20(-14)	9.59(-12)	1.50(-14)
80.	1.24(-11)	1.74(-12)	6.84(-14)	1.27(-11)	2.74(-14)
90.	1.56(-11)	2.62(-12)	1.25(-13)	1.59(-11)	4.48(-14)
100.	1.88(-11)	3.68(-12)	2.06(-13)	1.92(-11)	6.76(-14)
110.	2.22(-11)	4.88(-12)	3.13(-13)	2.26(-11)	9.61(-14)
120.	2.56(-11)	6.22(-12)	4.47(-13)	2.61(-11)	1.31(-13)
130.	2.90(-11)	7.68(-12)	6.10(-13)	2.96(-11)	1.71(-13)
140.	3.25(-11)	9.25(-12)	8.01(-13)	3.31(-11)	2.17(-13)
150.	3.60(-11)	1.09(-11)	1.02(-12)	3.66(-11)	2.70(-13)
160.	3.95(-11)	1.26(-11)	1.27(-12)	4.02(-11)	3.28(-13)
170.	4.30(-11)	1.44(-11)	1.54(-12)	4.37(-11)	3.92(-13)
180.	4.65(-11)	1.63(-11)	1.84(-12)	4.73(-11)	4.61(-13)
190.	5.00(-11)	1.82(-11)	2.17(-12)	5.09(-11)	5.36(-13)
200.	5.34(-11)	2.02(-11)	2.52(-12)	5.44(-11)	6.16(-13)
220.	6.04(-11)	2.42(-11)	3.29(-12)	6.15(-11)	7.90(-13)
240.	6.72(-11)	2.83(-11)	4.15(-12)	6.85(-11)	9.82(-13)
260.	7.40(-11)	3.24(-11)	5.09(-12)	7.54(-11)	1.19)-11)
280.	8.07(-11)	3.66(-11)	6.11(-12)	8.23(-11)	1.41(-12)
300.	8.73(-11)	4.09(-11)	7.19(-12)	8.90(-11)	1.65(-12)

T(K)	1,0 → 1,2	0,0 → 1,2	2,0 → 0,2	1,0 → 0,2	0,0 → 0,2
10.	1.32(-35)	1.79(-41)	2.53(-20)	3.12(-30)	1.13(-35)
20.	1.48(-23)	1.20(-26)	1.26(-17)	5.75(-22)	1.23(-23)
30.	7.54(-20)	5.18(-22)	1.13(-16)	3.67(-19)	6.19(-20)
40.	5.66(-18)	1.14(-19)	3.82(-16)	1.03(-17)	4.61(-18)
50.	7.84(-17)	3.02(-18)	8.86(-16)	8.24(-17)	6.34(-17)
60.	4.64(-16)	2.79(-17)	1.68(-15)	3.47(-16)	3.74(-16)
70.	1.68(-15)	1.40(-16)	2.82(-15)	1.00(-15)	1.35(-15)
80.	4.51(-15)	4.83(-16)	4.40(-15)	2.28(-15)	3.59(-15)
90.	9.82(-15)	1.29(-15)	6.48(-15)	4.43(-15)	7.77(-15)
100.	1.85(-14)	2.86(-15)	9.15(-15)	7.67(-15)	1.46(-14)
110.	3.14(-14)	5.58(-15)	1.25(-14)	1.22(-14)	2.45(-14)
120.	4.91(-14)	9.86(-15)	1.65(-14)	1.82(-14)	3.82(-14)
130.	7.22(-14)	1.61(-14)	2.12(-14)	2.58(-14)	5.58(-14)
140.	1.01(-13)	2.47(-14)	2.67(-14)	3.51(-14)	7.77(-14)
150.	1.36(-13)	3.62(-14)	3.30(-14)	4.62(-14)	1.04(-13)
160.	1.77(-13)	5.07(-14)	4.01(-14)	5.91(-14)	1.35(-13)
170.	2.24(-13)	6.87(-14)	4.81(-14)	7.39(-14)	1.70(-13)
180.	2.78(-13)	9.05(-14)	5.68(-14)	9.06(-14)	2.10(-13)
190.	3.37(-13)	1.16(-13)	6.64(-14)	1.09(-13)	2.54(-13)
200.	4.03(-13)	1.46(-13)	7.69(-14)	1.30(-13)	3.02(-13)
220.	5.51(-13)	2.20(-13)	1.00(-13)	1.76(-13)	4.10(-13)
240.	7.20(-13)	3.12(-13)	1.27(-13)	2.29(-13)	5.33(-13)
260.	9.08(-13)	4.23(-13)	1.57(-13)	2.90(-13)	6.69(-13)
280.	1.11(-12)	5.54(-13)	1.91(-13)	3.56(-13)	8.17(-13)
300.	1.34(-12)	7.04(-13)	2.28(-13)	4.28(-13)	9.75(-13)

TABLE 7. *Rotational de-excitation cross sections of HD and ortho-H2 ($j'_1\ j'_2 \rightarrow j_1\ j_2$) in units of* 10^{-16} cm^2 vs. *relative center of mass velocities; *: calculated.*

v(m/s)	1,1 → 0,1	2,1 → 1,1	2,1 → 0,1	0,3 → 0,1	0,3 → 1,1
30.	4.65(+1)	3.64(+1)	2.98(+0)	1.72(-1)	5.40(-2)
40.	7.60(+1)	*5.94(+1)	*4.86(+0)	2.82(-1)	8.82(-2)
60.	1.74(+2)	*2.52(+2)	1.13(+1)	6.45(-1)	2.02(-1)
80.	7.30(+1)	*6.28(+1)	*3.88(+0)	2.71(-1)	8.48(-2)
100.	*2.84(+1)	*4.99(+1)	*2.36(+0)	*1.05(-1)	*3.30(-2)
120.	2.09(+1)	3.40(+1)	1.70(+0)	7.77(-2)	2.43(-2)
150.	1.23(+1)	1.71(+1)	9.74(-1)	4.60(-2)	1.44(-2)
180.	8.81(+0)	*9.82(+0)	*6.76(-1)	3.34(-2)	1.04(-2)
210.	7.73(+0)	8.58(+0)	5.88(-1)	2.96(-2)	9.20(-3)
240.	9.58(+0)	1.06(+1)	7.21(-1)	3.71(-2)	1.15(-2)
270.	1.10(+1)	*1.21(+1)	*8.20(-1)	4.32(-2)	1.34(-2)
300.	8.24(+0)	9.05(+0)	6.16(-1)	3.28(-2)	1.01(-2)
360.	4.74(+0)	5.23(+0)	3.58(-1)	1.95(-2)	5.97(-3)
450.	*3.82(+0)	*4.24(+0)	*2.93(-1)	*1.66(-2)	*5.03(-3)
520.	2.99(+0)	3.34(+0)	2.32(-1)	1.33(-2)	4.08(-3)
600.	2.53(+0)	2.85(+0)	2.00(-1)	1.15(-2)	3.62(-3)
620.				*1.12(-2)	*3.52(-3)
800.	1.90(+0)	2.19(+0)	1.58(-1)	9.56(-3)	3.16(-3)
1200.	*1.55(+0)	1.90(+0)	1.47(-1)	*9.88(-3)	*3.62(-3)
1403.		*1.97(+0)	*1.58(-1)	*1.02(-2)	4.68(-3)
1500.	*1.55(+0)	1.99(+0)	*1.62(-1)	*1.07(-2)	*5.32(-3)
1791.				*1.25(-2)	*7.34(-3)
2004.	1.67(+0)	2.17(+0)	1.96(-1)	*1.42(-2)	*9.33(-3)
2300.	1.79(+0)	2.34(+0)	2.27(-1)	1.69(-2)	1.28(-2)
2592.		*2.52(+0)	*2.63(-1)		
2900.	2.06(+0)	2.68(+0)	2.97(-1)	2.43(-2)	2.25(-2)
3089.		*2.77(+0)	*3.20(-1)		
3200.	*2.20(+0)	2.82(+0)	3.31(-1)	*2.89(-2)	*2.89(-2)
3450.	*2.30(+0)	2.94(+0)	3.60(-1)	3.14(-2)	3.62(-2)

v(m/s)	1,1 → 0,1	2,1 → 1,1	2,1 → 0,1	0,3 → 0,1	0,3 → 1,1
3465.				*3.16(-2)	*3.66(-2)
3600.	2.36(+0)	3.00(+0)	3.76(-1)	3.35(-2)	4.00(-2)
3724.	*2.40(+0)				
4000.	2.48(+0)	3.13(+0)	4.22(-1)	3.97(-2)	5.11(-2)
4283.		*3.20(+0)	*4.54(-1)		
4500.	2.60(+0)	3.24(+0)	4.76(-1)	4.80(-2)	6.64(-2)
4676.	*2.63(+0)				
5000.	2.65(+0)	3.30(+0)	5.23(-1)	5.66(-2)	8.29(-2)
5113.				*5.85(-2)	*8.68(-2)
5500.	2.65(+0)	3.29(+0)	5.64(-1)	6.34(-2)	1.01(-1)
5699.		*3.27(+0)	*5.80(-1)		
6000.	*2.61(+0)	3.24(+0)	*5.98(-1)	6.93(-2)	1.19(-1)
6145.				*7.10(-2)	*1.24(-1)
6600.	2.51(+0)	3.24(+0)	6.28(-1)	7.59(-2)	1.41(-1)
6641.		*3.14(+0)	*6.30(-1)		
6901.	*2.46(+0)				
7300.	2.37(+0)	2.99(+0)	6.58(-1)	8.31(-2)	1.65(-1)

TABLE 7. *(Continued)*

v(m/s)	0,3 → 2,1	1,3 → 0,3	1,3 → 0,1	1,3 → 1,1	1,3 → 2,1
30.	1.38(-2)	4.68(+1)	7.05(-2)	2.71(-1)	4.51(-2)
40.	2.25(-2)	7.64(+1)	1.15(-1)	4.43(-1)	7.36(-2)
60.	5.15(-2)	1.75(+2)	2.64(-1)	1.02(+0)	1.69(-1)
80.	2.16(-2)	7.35(+1)	1.11(-1)	4.26(-1)	7.08(-2)
100.	8.41(-3)	*2.86(+1)	*4.31(-2)	*1.66(-1)	*2.76(-2)
120.	6.17(-3)	2.10(+1)	3.16(-2)	1.22(-1)	2.01(-2)
150.	3.62(-3)	1.23(+1)	1.85(-2)	7.11(-2)	1.17(-2)
180.	2.59(-3)	8.86(+0)	1.32(-2)	5.08(-2)	8.35(-3)
210.	2.27(-3)	7.78(+0)	1.15(-2)	4.42(-2)	7.24(-3)
240.	2.80(-3)	9.63(+0)	1.41(-2)	5.43(-2)	8.84(-3)
270.	3.20(-3)	1.11(+1)	1.61(-2)	6.19(-2)	1.00(-2)
300.	2.39(-3)	8.28(+0)	1.19(-2)	4.58(-2)	7.35(-3)
360.	1.36(-3)	4.76(+0)	6.73(-3)	2.58(-2)	4.05(-3)
450.	1.08(-3)	*3.84(+0)	*5.21(-3)	*1.99(-2)	*3.01(-3)
520.	8.43(-4)	3.01(+0)	4.25(-3)	1.64(-2)	2.64(-3)
530.		*2.93(+0)	*4.16(-3)	*1.60(-2)	*2.61(-3)
600.	7.13(-4)	2.54(+0)	3.72(-3)	1.43(-2)	2.41(-3)
620.	*6.86(-4)				
695.		*2.16(+0)	*3.30(-3)	*1.27(-2)	*2.24(-3)
800.	6.24(-4)	1.91(+0)	3.04(-3)	1.17(-2)	2.01(-3)
1200.	7.32(-4)	*1.56(+0)	*3.02(-3)	*1.16(-2)	*1.77(-3)
1403.	*8.74(-4)	1.55(+0)	3.38(-3)	1.29(-2)	2.00(-3)
1500.	9.74(-4)	*1.56(+0)	*3.62(-3)	*1.37(-2)	*2.15(-3)
1791.	*1.35(-3)				
2004.	*1.78(-3)	1.68(+0)	5.43(-3)	1.84(-2)	*4.52(-3)
2300.	3.08(-3)	1.79(+0)	7.01(-3)	2.24(-2)	6.56(-3)
2900.	6.85(-3)	2.04(+0)	1.14(-2)	3.36(-2)	1.24(-2)
2911.		*2.05(+0)	*1.15(-2)	*3.39(-2)	
3200.	9.37(-3)	*2.19(+0)	*1.44(-2)	*3.92(-2)	*1.62(-2)

v(m/s)	0,3 → 2,1	1,3 → 0,3	1,3 → 0,1	1,3 → 1,1	1,3 → 2,1
3450.	*1.18(-2)	2.28(+0)	1.70(-2)	4.37(-2)	1.98(-2)
3465.	*1.20(-2)				
3600.	1.40(-2)	2.33(+0)	1.87(-2)	4.63(-2)	2.20(-2)
4000.	2.07(-2)	2.43(+0)	2.36(-2)	5.38(-2)	2.88(-2)
4500.	3.03(-2)	2.50(+0)	3.04(-2)	6.35(-2)	3.82(-2)
4937.		*2.52(+0)	*3.67(-2)	*7.22(-2)	
5000.	4.10(-2)	2.53(+0)	3.77(-2)	7.36(-2)	4.84(-2)
5500.	5.24(-2)	2.58(+0)	4.62(-2)	8.50(-2)	5.90(-2)
6000.	*6.39(-2)	*2.60(+0)	*5.47(-2)	*9.61(-2)	*6.96(-2)
6145.	*6.73(-2)				
6600.	7.77(-2)	2.58(+0)	6.48(-2)	1.09(-1)	8.22(-2)
7300.	9.35(-2)	2.53(+0)	5.44(-1)	1.23(-1)	9.64(-2)

TABLE 8. *Rotational de-excitation rate coefficients of HD and ortho-H2 ($j_1' j_2' \rightarrow j_1 j_2$) in* $cm^3 sec^{-1}$ *units.*

T(K)	1,1 → 0,1	2,1 → 1,1	2,1 → 0,1	0,3 → 0,1	0,3 → 1,1
10.	1.89(-11)	2.14(-11)	1.44(-12)	7.88(-14)	2.45(-14)
20.	1.72(-11)	1.96(-11)	1.36(-12)	7.85(-14)	2.52(-14)
30.	1.70(-11)	1.97(-11)	1.41(-12)	8.42(-14)	2.87(-14)
40.	1.75(-11)	2.05(-11)	1.51(-12)	9.26(-14)	3.41(-14)
50.	1.82(-11)	2.17(-11)	1.63(-12)	1.03(-13)	4.09(-14)
60.	1.90(-11)	2.30(-11)	1.77(-12)	1.14(-13)	4.90(-14)
70.	2.00(-11)	2.44(-11)	1.92(-12)	1.26(-13)	5.84(-14)
80.	2.10(-11)	2.58(-11)	2.08(-12)	1.38(-13)	6.89(-14)
90.	2.21(-11)	2.73(-11)	2.24(-12)	1.51(-13)	8.05(-14)
100.	2.31(-11)	2.88(-11)	2.42(-12)	1.65(-13)	9.32(-14)
110.	2.42(-11)	3.04(-11)	2.60(-12)	1.80(-13)	1.07(-13)
120.	2.54(-11)	3.19(-11)	2.78(-12)	1.95(-13)	1.22(-13)
130.	2.65(-11)	3.35(-11)	2.96(-12)	2.11(-13)	1.38(-13)
140.	2.76(-11)	3.50(-11)	3.16(-12)	2.28(-13)	1.55(-13)
150.	2.88(-11)	3.66(-11)	3.35(-12)	2.44(-13)	1.73(-13)
160.	3.00(-11)	3.82(-11)	3.55(-12)	2.62(-13)	1.92(-13)
170.	3.11(-11)	3.97(-11)	3.75(-12)	2.79(-13)	2.12(-13)
180.	3.23(-11)	4.12(-11)	3.95(-12)	2.98(-13)	2.33(-13)
190.	3.34(-11)	4.28(-11)	4.15(-12)	3.16(-13)	2.54(-13)
200.	3.46(-11)	4.43(-11)	4.36(-12)	3.35(-13)	2.77(-13)
220.	3.69(-11)	4.73(-11)	4.77(-12)	3.74(-13)	3.25(-13)
240.	3.92(-11)	5.02(-11)	5.19(-12)	4.13(-13)	3.76(-13)
260.	4.14(-11)	5.31(-11)	5.61(-12)	4.54(-13)	4.30(-13)
280.	4.36(-11)	5.60(-11)	6.03(-12)	4.96(-13)	4.86(-13)
300.	4.58(-11)	5.87(-11)	6.46(-12)	5.39(-13)	5.46(-13)

T(K)	0,3 → 2,1	1,3 → 0,3	1,3 → 0,1	1,3 → 1,1	1,3 → 2,1
10.	5.47(-15)	1.89(-11)	2.74(-14)	1.05(-13)	1.70(-14)
20.	5.30(-15)	1.72(-11)	2.60(-14)	9.99(-14)	1.64(-14)
30.	5.85(-15)	1.71(-11)	2.74(-14)	1.05(-13)	1.72(-14)
40.	6.80(-15)	1.75(-11)	3.02(-14)	1.15(-13)	1.91(-14)
50.	8.08(-15)	1.83(-11)	3.38(-14)	1.28(-13)	2.17(-14)
60.	9.72(-15)	1.91(-11)	3.80(-14)	1.42(-13)	2.52(-14)
70.	1.17(-14)	2.01(-11)	4.28(-14)	1.58(-13)	2.94(-14)
80.	1.42(-14)	2.11(-11)	4.82(-14)	1.75(-13)	3.44(-14)
90.	1.71(-14)	2.21(-11)	5.40(-14)	1.93(-13)	4.01(-14)
100.	2.04(-14)	2.32(-11)	6.04(-14)	2.12(-13)	4.66(-14)
110.	2.42(-14)	2.43(-11)	6.73(-14)	2.32(-13)	5.38(-14)
120.	2.85(-14)	2.54(-11)	7.46(-14)	2.53(-13)	6.16(-14)
130.	3.33(-14)	2.66(-11)	8.24(-14)	2.75(-13)	7.02(-14)
140.	3.86(-14)	2.77(-11)	9.06(-14)	2.97(-13)	7.94(-14)
150.	4.44(-14)	2.88(-11)	9.92(-14)	3.21(-13)	8.92(-14)
160.	5.07(-14)	3.00(-11)	1.08(-13)	3.45(-13)	9.97(-14)
170.	5.75(-14)	3.11(-11)	1.18(-13)	3.69(-13)	1.11(-13)
180.	6.48(-14)	3.23(-11)	1.28(-13)	3.94(-13)	1.22(-13)
190.	7.27(-14)	3.34(-11)	1.38(-13)	4.20(-13)	1.34(-13)
200.	8.10(-14)	3.46(-11)	1.48(-13)	4.46(-13)	1.47(-13)
220.	9.91(-14)	3.68(-11)	1.70(-13)	4.99(-13)	1.74(-13)
240.	1.19(-13)	3.90(-11)	1.94(-13)	5.54(-13)	2.03(-13)
260.	1.41(-13)	4.12(-11)	2.19(-13)	6.10(-13)	2.34(-13)
280.	1.65(-13)	4.34(-11)	2.45(-13)	6.67(-13)	2.66(-13)
300.	1.91(-13)	4.55(-11)	2.72(-13)	7.25(-13)	3.00(-13)

TABLE 9. *Rotational excitation rate coefficients of HD and para-H2* $(j_1' j_2' \rightarrow j_1 j_2)$ *in* $cm^3 sec^{-1}$ *units.*

T(K)	0,1 → 1,1	1,1 → 2,1	0,1 → 2,1	0,1 → 0,3	1,1 → 0,3
10.	1.50(-16)	2.74(-22)	1.47(-28)	3.81(-51)	1.49(-46)
20.	8.39(-14)	9.04(-17)	3.08(-20)	8.34(-32)	5.48(-30)
30.	7.07(-13)	6.47(-15)	1.92(-17)	1.16(-25)	9.55(-25)
40.	2.11(-12)	5.69(-14)	5.06(-16)	1.46(-22)	4.43(-22)
50.	4.18(-12)	2.16(-13)	3.74(-15)	1.10(-20)	1.91(-20)
60.	6.72(-12)	5.38(-13)	1.46(-14)	2.04(-19)	2.49(-19)
70.	9.58(-12)	1.05(-12)	3.96(-14)	1.68(-18)	1.63(-18)
80.	1.27(-11)	1.76(-12)	8.52(-14)	8.37(-18)	6.93(-18)
90.	1.59(-11)	2.65(-12)	1.57(-13)	2.97(-17)	2.19(-17)
100.	1.92(-11)	3.72(-12)	2.59(-13)	8.28(-17)	5.62(-17)
110.	2.26(-11)	4.94(-12)	3.94(-13)	1.94(-16)	1.24(-16)
120.	2.61(-11)	6.31(-12)	5.65(-13)	4.00(-16)	2.42(-16)
130.	2.96(-11)	7.80(-12)	7.71(-13)	7.42(-16)	4.34(-16)
140.	3.32(-11)	9.39(-12)	1.01(-12)	1.27(-15)	7.22(-16)
150.	3.67(-11)	1.11(-11)	1.29(-12)	2.04(-15)	1.13(-15)
160.	4.03(-11)	1.28(-11)	1.61(-12)	3.11(-15)	1.70(-15)
170.	4.39(-11)	1.47(-11)	1.95(-12)	4.53(-15)	2.44(-15)
180.	4.74(-11)	1.66(-11)	2.33(-12)	6.36(-15)	3.38(-15)
190.	5.10(-11)	1.85(-11)	2.75(-12)	8.65(-15)	4.56(-15)
200.	5.46(-11)	2.05(-11)	3.19(-12)	1.14(-14)	6.00(-15)
220.	6.17(-11)	2.46(-11)	4.16(-12)	1.87(-14)	9.74(-15)
240.	6.88(-11)	2.88(-11)	5.23(-12)	2.86(-14)	1.48(-14)
260.	7.58(-11)	3.31(-11)	6.40(-12)	4.12(-14)	2.13(-14)
280.	8.28(-11)	3.74(-11)	7.64(-12)	5.67(-14)	2.93(-14)
300.	8.96(-11)	4.17(-11)	8.96(-12)	7.53(-14)	3.90(-14)

T(K)	2,1 → 0,3	0,3 → 1,3	0,1 → 1,3	1,1 → 1,3	2,1 → 1,3
10.	2.59(-36)	1.51(-16)	1.05(-56)	5.09(-51)	6.42(-41)
20.	2.49(-25)	8.43(-14)	1.35(-35)	1.06(-31)	3.76(-27)
30.	5.91(-22)	7.10(-13)	1.57(-27)	1.45(-25)	7.24(-23)
40.	3.18(-20)	2.12(-12)	5.75(-24)	1.81(-22)	1.08(-20)
50.	3.78(-19)	4.20(-12)	8.35(-22)	1.37(-20)	2.34(-19)
60.	2.11(-18)	6.75(-12)	2.41(-20)	2.55(-19)	1.93(-18)
70.	7.63(-18)	9.62(-12)	2.75(-19)	2.12(-18)	9.15(-18)
80.	2.10(-17)	1.27(-11)	1.76(-18)	1.06(-17)	3.06(-17)
90.	4.78(-17)	1.60(-11)	7.63(-18)	3.78(-17)	8.10(-17)
100.	9.54(-17)	1.93(-11)	2.51(-17)	1.06(-16)	1.81(-16)
110.	1.72(-16)	2.27(-11)	6.78(-17)	2.50(-16)	3.57(-16)
120.	2.87(-16)	2.62(-11)	1.57(-16)	5.18(-16)	6.39(-16)
130.	4.51(-16)	2.97(-11)	3.24(-16)	9.66(-16)	1.06(-15)
140.	6.73(-16)	3.32(-11)	6.08(-16)	1.66(-15)	1.66(-15)
150.	9.64(-15)	3.68(-11)	1.06(-15)	2.68(-15)	2.47(-15)
160.	1.33(-15)	4.03(-11)	1.73(-15)	4.10(-15)	3.52(-15)
170.	1.79(-15)	4.39(-11)	2.69(-15)	5.99(-15)	4.86(-15)
180.	2.34(-15)	4.75(-11)	4.01(-15)	8.43(-15)	6.50(-15)
190.	3.01(-15)	5.10(-11)	5.76(-15)	1.15(-14)	8.49(-15)
200.	3.78(-15)	5.46(-11)	8.00(-15)	1.52(-14)	1.08(-14)
220.	5.71(-15)	6.16(-11)	1.43(-14)	2.50(-14)	1.68(-14)
240.	8.17(-15)	6.86(-11)	2.36(-14)	3.83(-14)	2.44(-14)
260.	1.12(-14)	7.55(-11)	3.63(-14)	5.52(-14)	3.40(-14)
280.	1.49(-14)	8.23(-11)	5.31(-14)	7.62(-14)	4.55(-14)
300.	1.92(-14)	8.90(-11)	7.43(-14)	1.01(-13)	5.90(-14)

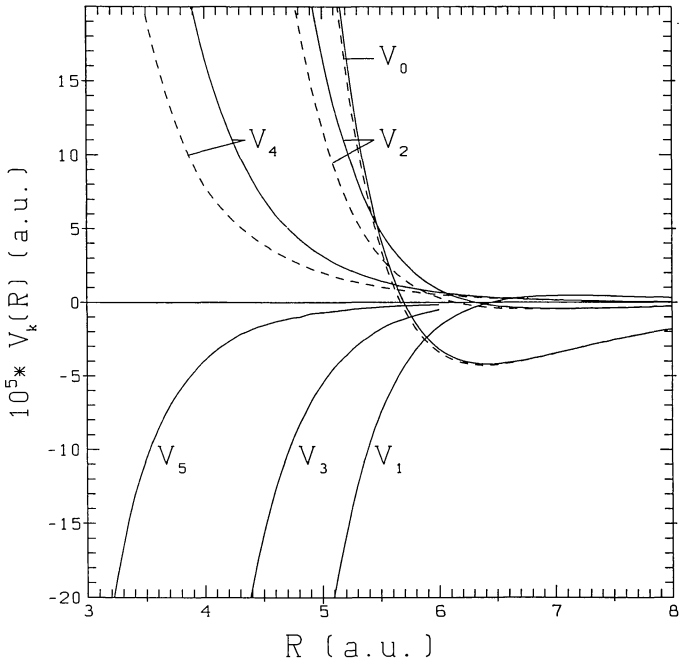

FIGURE 1. Potential terms V_λ of the HD-He interaction potential expanded in Legendre polynomials. The three dashed curves show the corresponding V_λ terms of the H2-He interaction. The intra-molecular distance parameter of both potentials is 1.449 a.u.

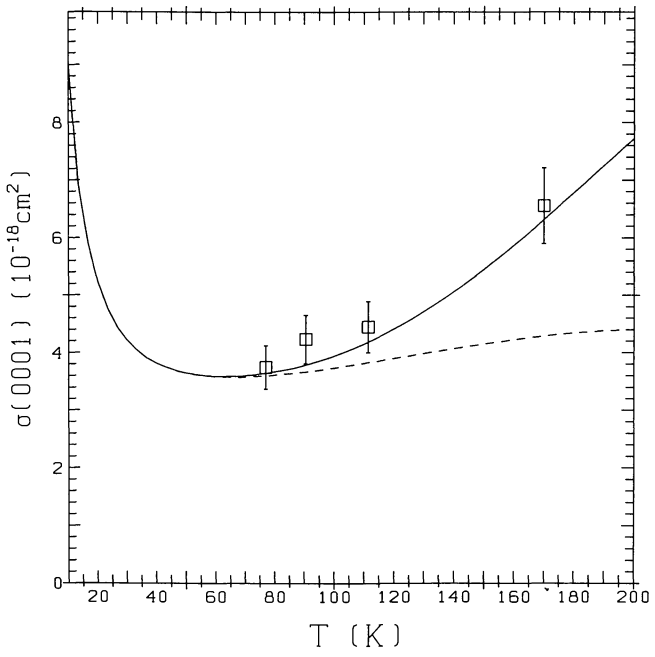

FIGURE 2. Comparison of rotational relaxation cross sections $\sigma(0001)$ of para-H2 derived from the F84 potential fit with measurements of Jonkman *et al.* (1968) (error bars drawn are ±10%). The dashed curve shows results of the "two-state approximation".

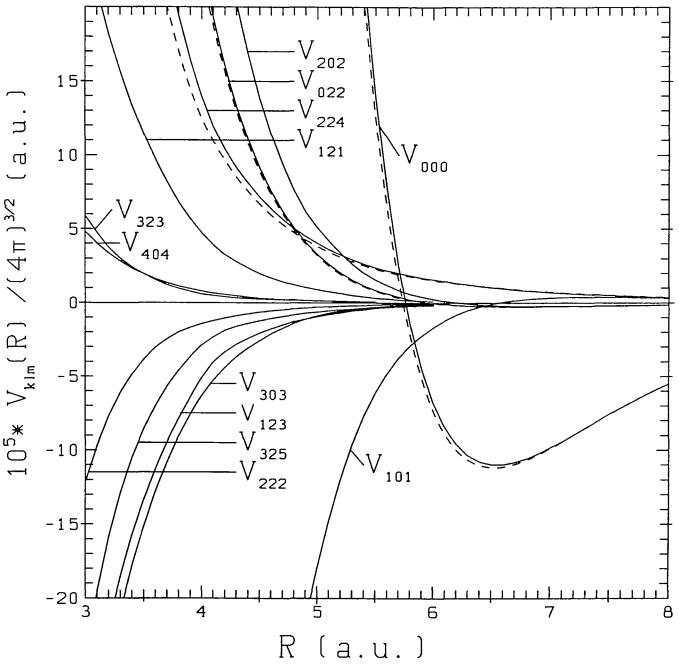

FIGURE 3. Expansion coefficient functions $V_{klm}(R)$ of the rigid rotor ($r_{HD} = r_{H2} = 1.449$a.u.) interaction potentials of HD-H2 and H2-H2 (dashed curves) obtained for a triple product expansion of spherical harmonics.

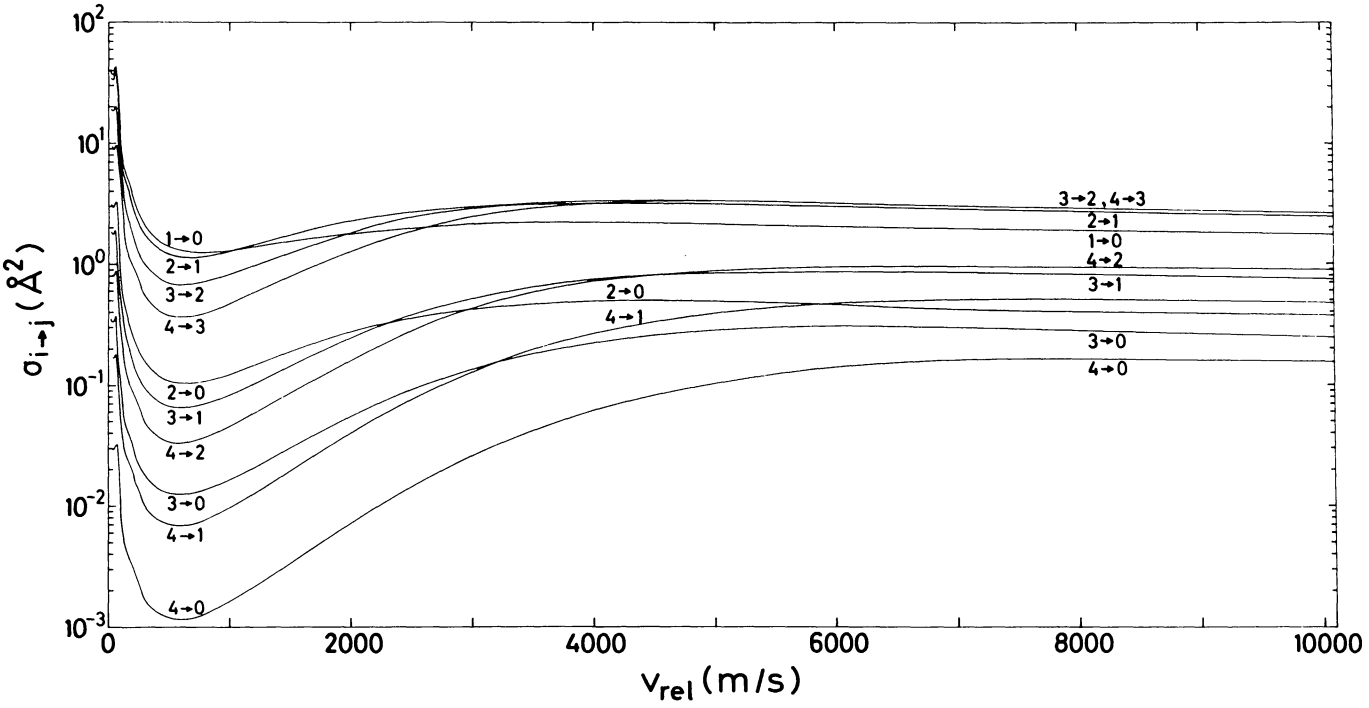

FIGURE 4. Calculated rotational de-excitation cross section curves of HD-He vs. relative velocity.

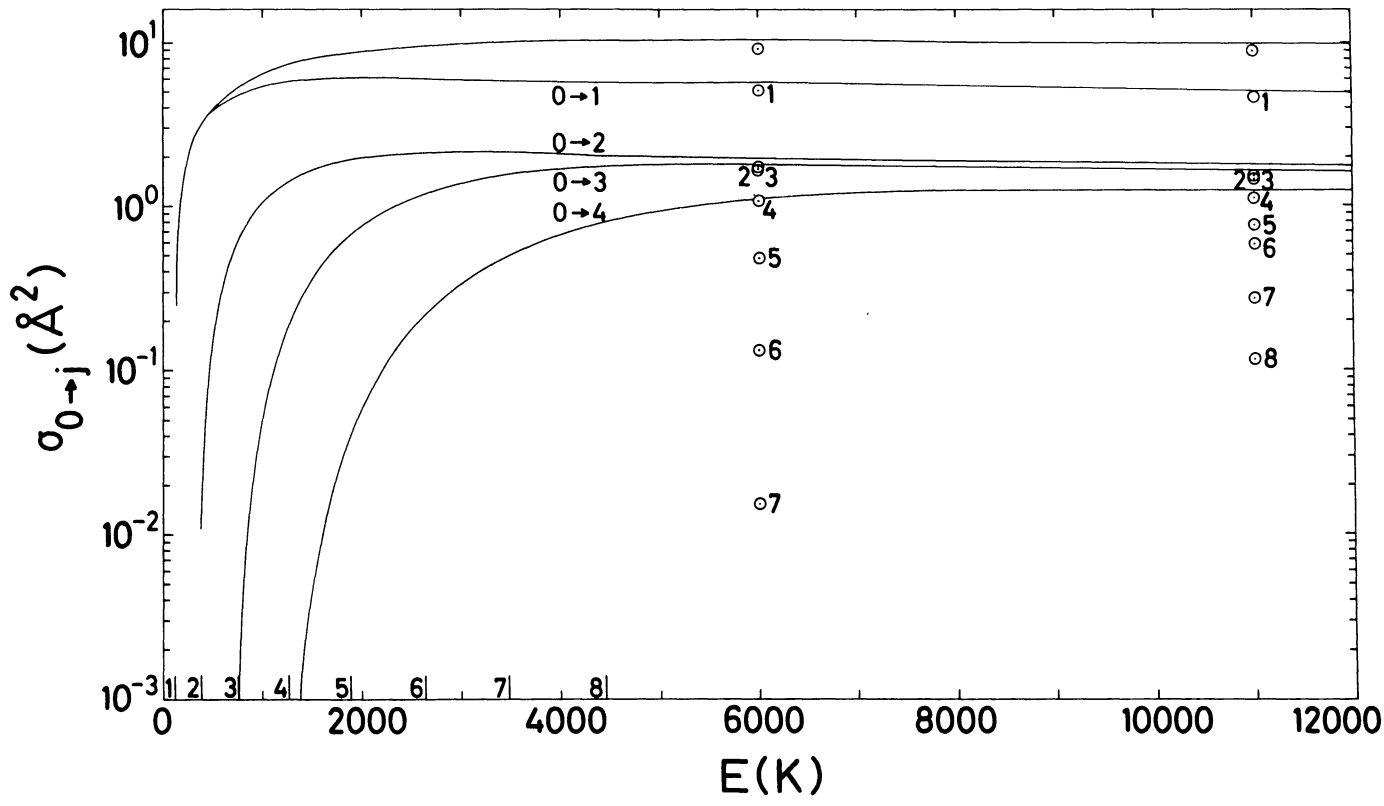

FIGURE 5. Calculated rotational excitation cross sections of HD-He for transitions from $j' = 0$ to j, each one obtained by using a basis set of rotational eigenfunctions ranging up to $j + 2$. The excitation thresholds are indicated by short vertical lines. Two extra sets of results (⊙) provide the corresponding (almost) converged cross sections obtained from a basis $j = 0$ to 8. The upper curve displays the sum over the inelastic cross sections.

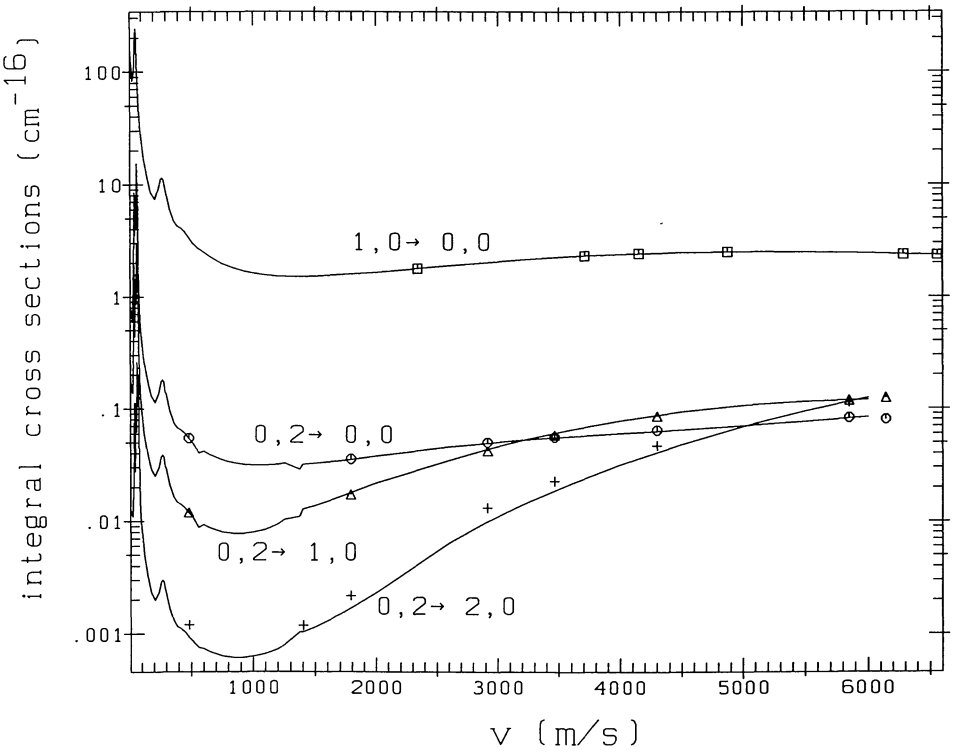

FIGURE 6. Calculated de-excitation cross sections of HD-H2 for transitions from j'_{HD}, $j'_{H2} = 1, 0$ and 0,2. The extra points on the curves are test results obtained from extended basis sets as explained in the text.

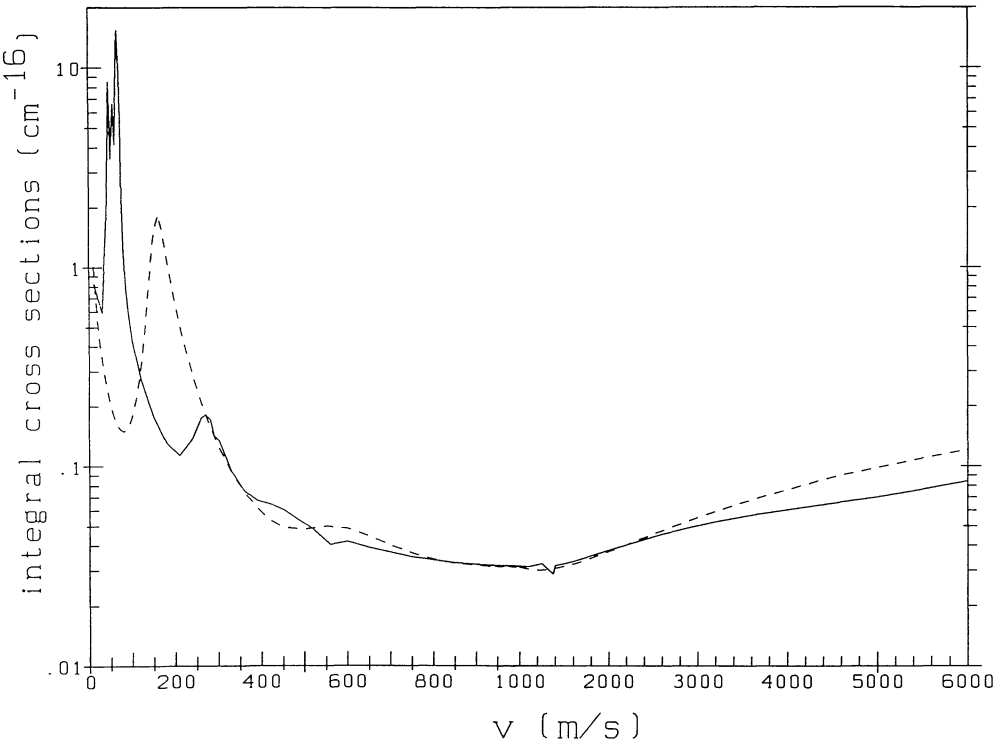

FIGURE 7. Comparison of the $\sigma_{0,2\to 0,0}$ cross sections of HD-H2 and symmetrized H2-H2 (dashed curve), derived from the same electronic PES. The first sixth of the velocity range has been enlarged in order to show the different resonance features. The small (calculated) bump of the HD-H2 cross section at 1375.m/s indicates resonance features close to the (1,2) excitation threshold at 1329.m/s.

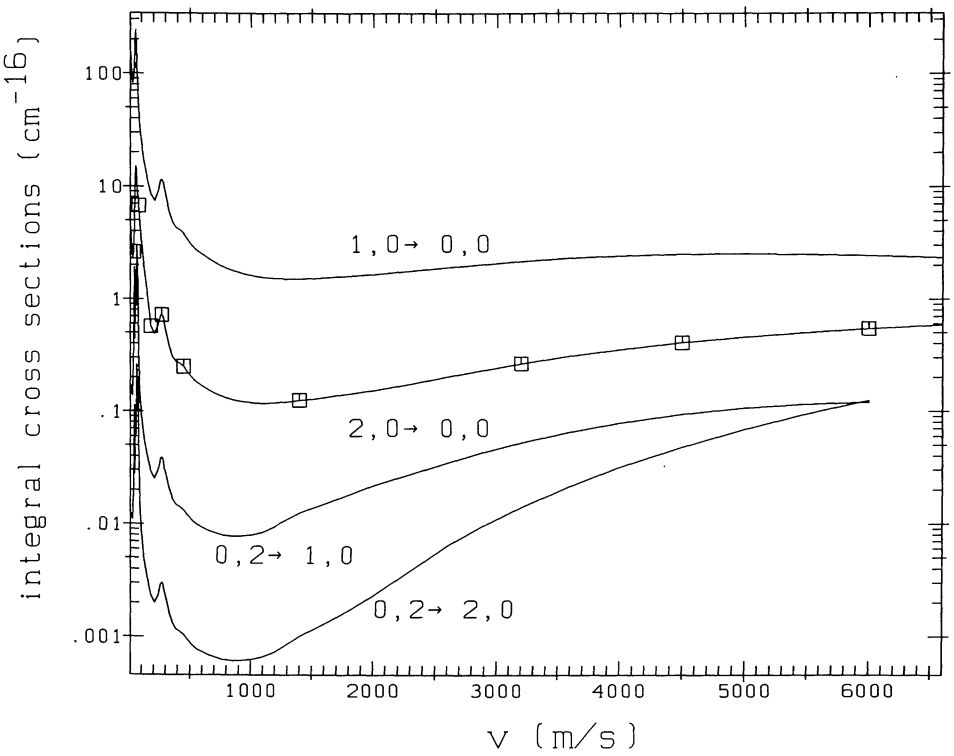

FIGURE 8. A demonstration of the interpolation procedure applied to the limitted sets of calculated cross sections: Nine points of the HD-H2 cross section $\sigma_{2,0\to0,0}$ vs. relative velocity have been completed to a reasonable dense grid by scaling of the $\sigma_{1,0\to0,0}$ cross section. Two other (smoothed) cross section curves available for this procedure should give slightly different results that could be used for error estimates.

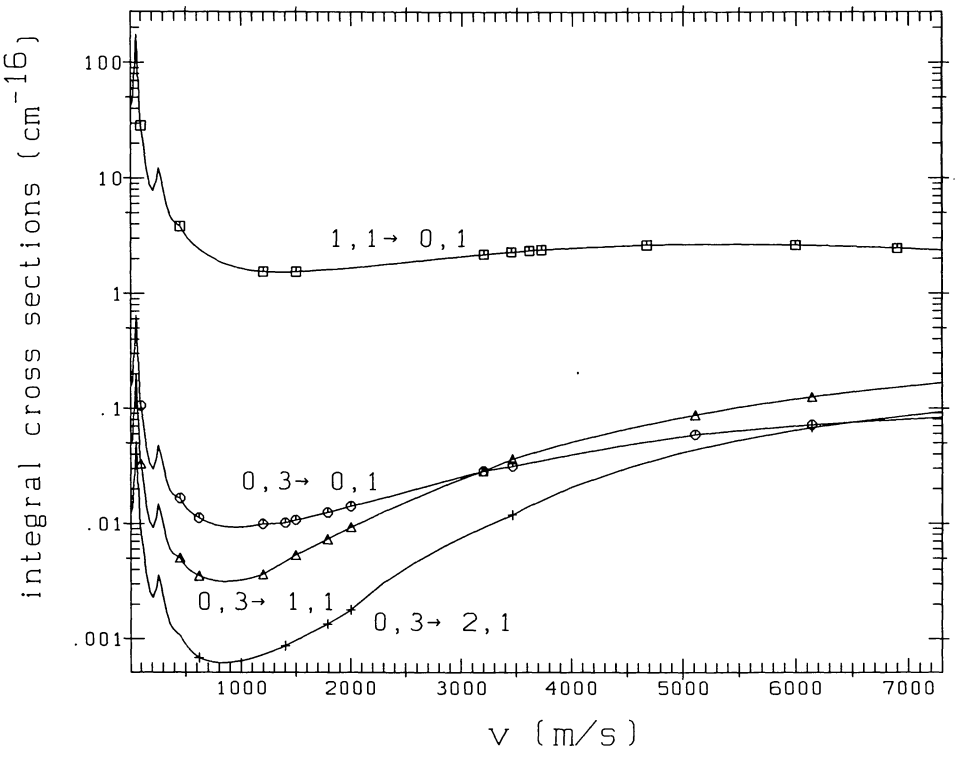

FIGURE 9. Calculated de-excitation cross sections of HD-H2 for transitions from j'_{HD}, $j'_{H2} = 1, 1$ and 0,3. The marked points on the cross section curves indicate results obtained from (almost) converged basis sets, with the exception of $\sigma_{0,3\to2,1}$.

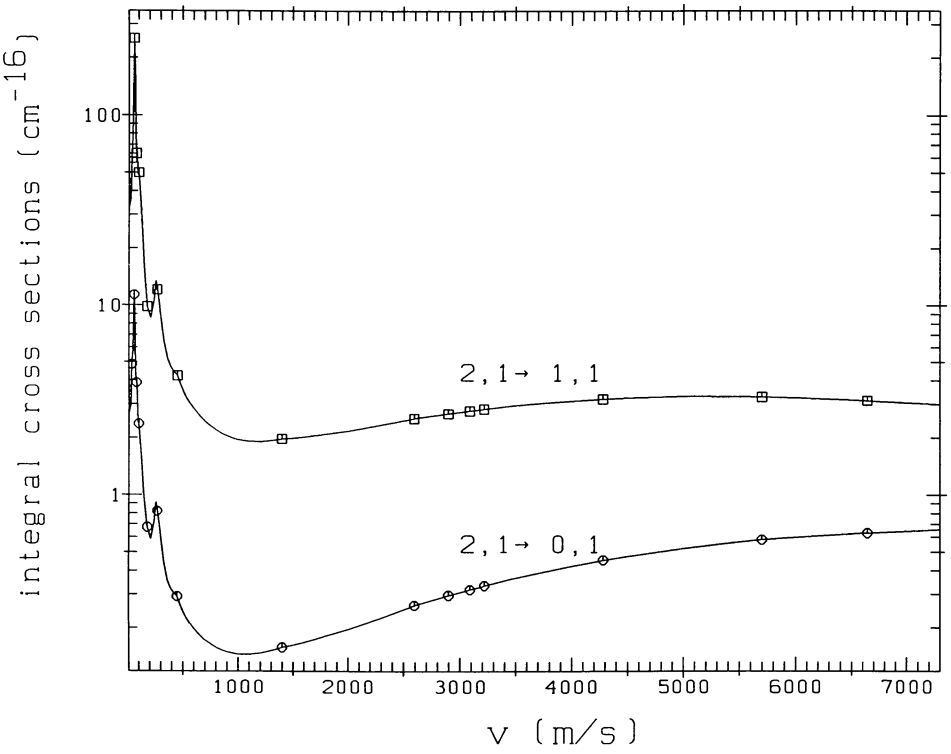

FIGURE 10. De-excitation cross sections $\sigma_{2,1\to1,1}$ and $\sigma_{2,1\to0,1}$ of HD-H2 calculated with the basis (IV) at the marked points and interpolated by scaling of $\sigma_{1,1\to0,1}$.

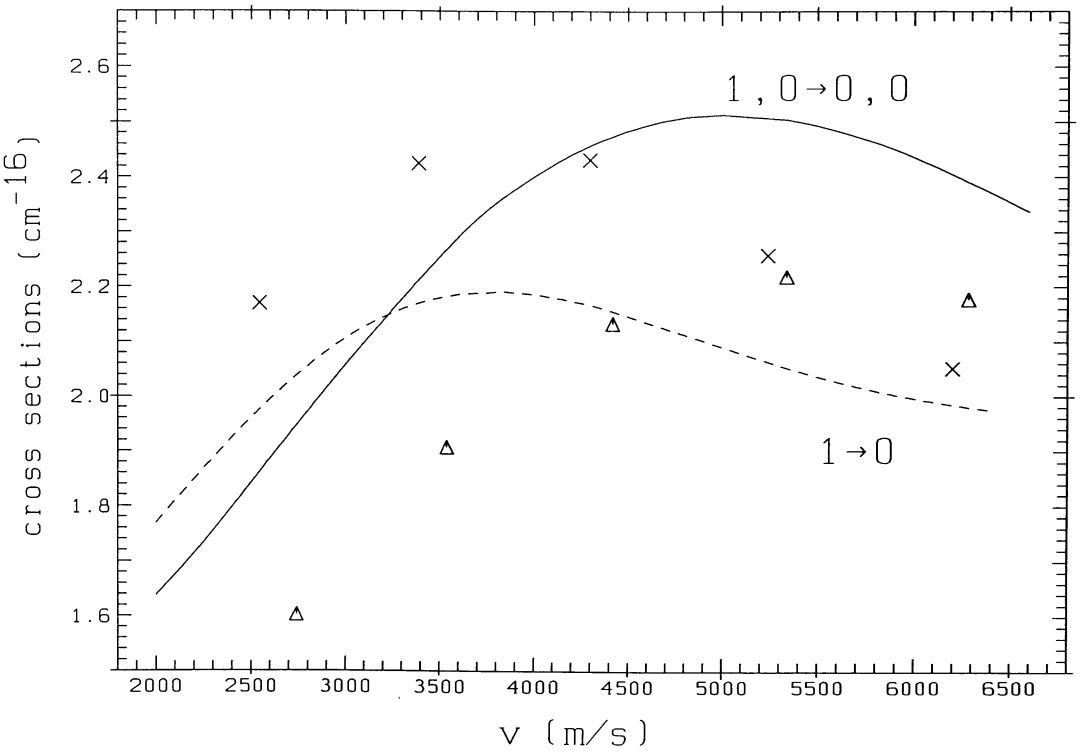

FIGURE 11. De-excitation cross sections of HD-H2 (solid line) and HD-He (dashed line) for a) $j_{HD} = 1 \to 0$ ($j_{H2} = 0$) and b) $j_{HD} = 2 \to 1$ ($j_{H2} = 0$) transitions. Δ : results obtained from the HD-H2 potential after scaling by 0.5; $\times$: results obtained by the same scaling of the HD-H2 potential and after replacing the H2 mass by the He mass.

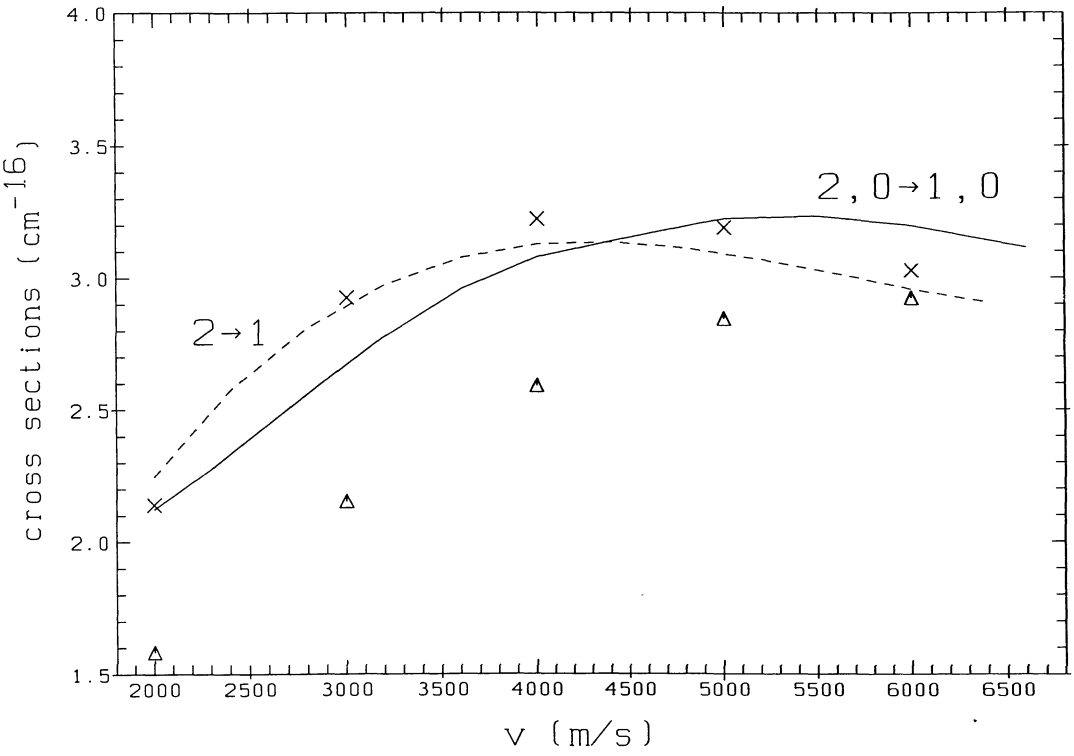

FIGURE 11. (*Continued*)

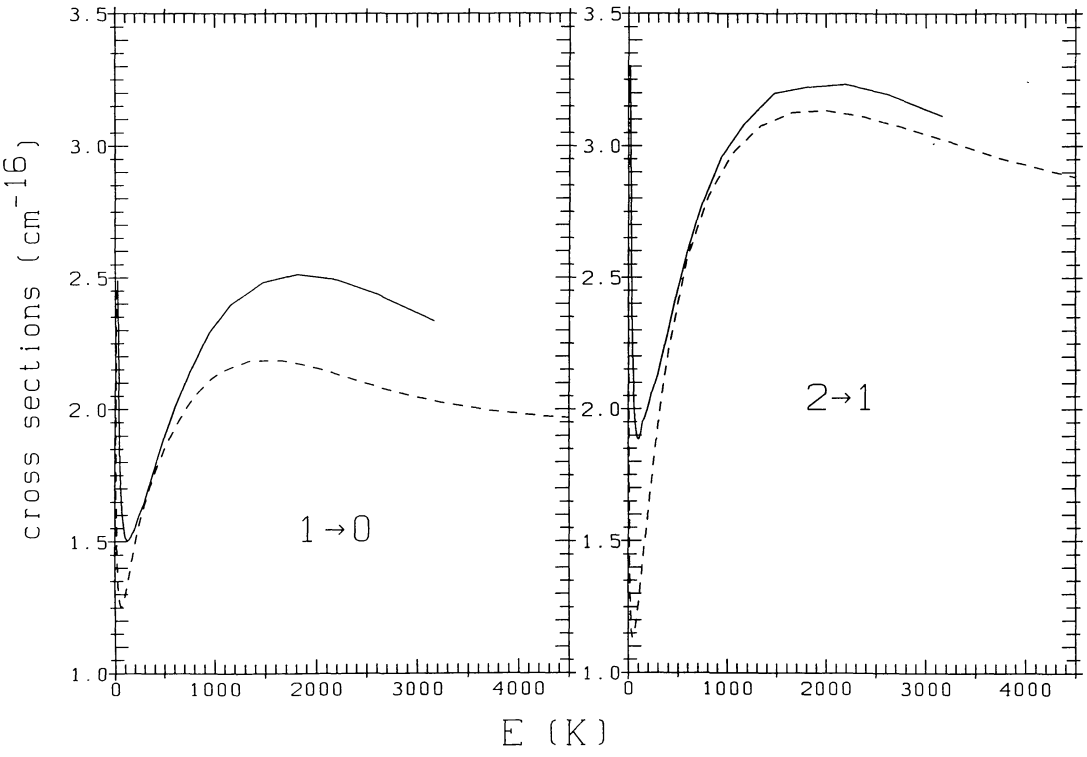

FIGURE 12. De-excitation cross sections vs. collision energy of HD-H2 (solid lines) and HD-He (dashed lines) for a) $j_{HD} = 1 \rightarrow 0$ ($j_{H2} = 0$) and b) $j_{HD} = 2 \rightarrow 1$ ($j_{H2} = 0$) transitions.

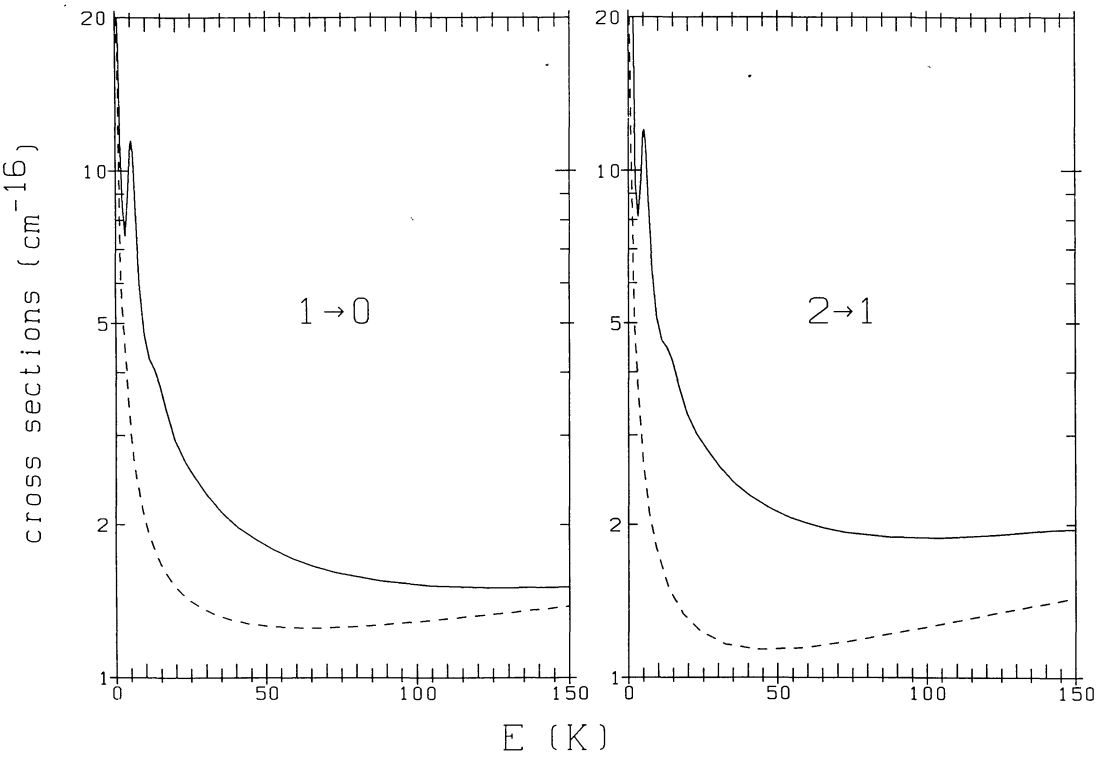

FIGURE 13. De-excitation cross sections of HD-H2 (solid line) and HD-He (dashed line) at very low collision energies, for a) $j_{HD} = 1 \rightarrow 0$ ($j_{H2} = 0$) and b) $j_{HD} = 2 \rightarrow 1$ ($j_{H2} = 0$) transitions. The very narrow $l = 1$ resonances of HD-He and the $l = 2$ resonances of HD-H2 have been left out.